Transactions of the Royal Society of Edinburgh: Earth Sciences, **83**, 327–345, 1992

To Scott,
with compliments,
Richard

The Cretaceous volcanic-plutonic province of the central Queensland (Australia) coast—a rift related 'calc-alkaline' province

A. Ewart, R. W. Schon and B. W. Chappell

ABSTRACT: Silicic and minor intermediate and mafic pyroclastics, lavas, and dykes occupy a NW-trending zone through the Whitsunday, Cumberland and Northumberland Island groups, and locally areas on the adjacent mainland, over a distance of more than 300 km along the central Queensland coast. K–Ar and Rb–Sr data indicate an age range of 95–132 Ma, with the main activity approximately between 105–120 Ma; there is, however, evidence for easterly increasing ages. Comagmatic granites, some clearly intrusive into the volcanics, occur together with two localised areas of Triassic potassic granites (229 Ma), that form the immediate basement.

The volcanics are dominantly rhyolitic to dacitic lithic ignimbrites, with intercalated surge and bedded tuffs, accretionary lapilli tuffs, and lag deposits. Associated rock types include isolated rhyolitic and dacitic domes, and volumetrically minor andesite and rare basalt flows. The sequence is cut by abundant dykes, especially in the northern region and adjacent mainland, ranging from dolerite through andesite, dacite and rhyolite. Dyke orientations show maxima between NW–NNE. Isotope data, similarities in petrography and mineralogy, and alteration patterns all suggest dyke intrusion to be broadly contemporaneous with volcanism. The thickness of the volcanics is unconstrained, although in the Whitsunday area, minimum thicknesses of >1 km are inferred. Eruptive centres are believed to occur throughout the region, and include at least two areas of caldera-style collapse. The sequences are thus considered as predominantly intracaldera.

The phenocryst mineralogy is similar to modern "orogenic" volcanics. Phases include plagioclase, augite, hypersthene (uralitised), magnetite, ilmenite, with less common hornblende, and even rarer quartz, sanidine, and biotite. Fe-enriched compositions only develop in some high-silica rhyolites. The granites range from quartz diorite to granite s.s., and some contain spectacular concentrations of partially disaggregated dioritic inclusions.

Chemically, the suite ranges continuously from basalt to high-silica rhyolite, with calc-alkali to high-K affinities, and geochemical signatures similar to modern subduction-related magmas. Only the high-silica rhyolites and granites exhibit evidence of extensive fractional crystallisation (e.g. pronounced Eu anomalies). Variation within the suite can only satisfactorily be modelled in terms of two component mixing, with superimposed crystal fractionation. Nd and Sr isotope compositions are relatively coherent, with ε_{Nd} +2·2 to +7·3, and I_{Sr} (calculated at 110 and 115 Ma) 0·7031–0·7044. These are relatively primitive, and imply mantle and/or newly accreted crustal magma sources.

The two end-members proposed are within-plate tholeiitic melt, and ?low-silica rhyolitic melts generated by partial fusion of Permian (to ?Carboniferous) arc and arc basement. The arc-like geochemistry is thus considered to be source inherited. The tectonic setting for Cretaceous volcanism is correlated with updoming and basin rifting during the early stages of continental breakup, culminating in the opening of the Tasman Basin. Cretaceous volcanism is also recognised in the Maryborough Basin (S Queensland), the Lord Howe Rise, and New Caledonia, indicating the regional extent of volcanism associated with the complex breakup of the eastern Australasian continent margin.

KEY WORDS: rifting, silicic volcanism, pyroclastics, isotopes, trace elements, Cretaceous, crustal evolution, SW Pacific.

The Lower Cretaceous igneous provinces of the central Queensland coast were first mapped by Clarke *et al.* (1971). The southeasterly extension of the volcanics and intrusives had been previously recorded by Jensen *et al.* (1966), but mapped as Tertiary in age. Clarke *et al.* (1971) divided the volcanics into two units, the Whitsunday and Prosperpine volcanics; the former were defined as the thick (>1000 m) sequence of felsic to intermediate pyroclastics and minor flows which form most of the off-shore islands in the Proserpine map sheet area (Fig. 1). These authors considered their depositional environment to be sub-aqueous, in a land-locked intramontane basin. The Prosperine Volcanics were defined as the thick (>1000 m) sequence of rhyolite flows and minor pyroclastics and andesite overlying Lower Permian volcanics (Airlie Volcanics) on the mainland coast, and regarded as the

terrestrial equivalents of the off-shore sequences, deposited on a relatively stable block of pre-existing volcanic basement

This study has confirmed the southeasterly extension of the Whitsunday volcanics to the Percy Islands (Fig. 1), a strike length of approximately 300 km. Moreover, Early Cretaceous intermediate-silicic volcanism is known further south, most notably in the Maryborough region (Ellis & Whitaker 1976) comprising the Grahams Creek Formation. Further off-shore extensions of ?Late Cretaceous volcanism are recorded in the wells of Wreck Is. and Capricorn 1A (see Fig. 17; Davies & Marshall in press), and imply an extensive off-shore zone of volcanism of at least 900 km length. Within the study areas, Clarke *et al.* (1971) recognised the existence of associated granites, presumed to be coeval with the silicic volcanics, together with abundant dykes ranging from mafic to silicic in compositions, that cut most of the granites and volcanics alike (Figs 1, 2). This study has confirmed the Cretaceous age of many of the granites, but has shown some to be Triassic, most notably those of the Shaw Is. and Knight Is. groups (Fig. 1). A further complication in the region is the extent of faulting (Fig. 2), including the possible existence of 90 km of lateral movement along the Cumberland fault

The main purpose of this paper is to present the first petrological and geochemical data on the Whitsunday Volcanics, a suite of dolerites, andesites, dacites and rhyolites, to interpret these data in terms of the tectonomagmatic affinities of the magmas, and to consider their significance in terms of the possible origin(s) of the magmas.

1. Tectonic environment

The Cretaceous was a period of intense plate divergence of East Gondwana which resulted in the isolation of the Australian continent, and the development of its modern outline (Veevers *et al.* 1991). Rifting along the modern eastern Australian coast is interpreted as commencing in the late Cretaceous (96 Ma), with separation underway by 84 Ma; termination of spreading within the Tasman Sea occurred by approximately 55 Ma (Veevers *et al.* 1991). The zone of divergence, however, did not pass close to the present eastern Queensland coast, having diverted eastwards along a transform fault, leaving the off-shore Queensland and Marian plateaux. The Whitsunday volcanics are situated along the western margin of the Marian Plateau (Falvey & Mutter 1981). These authors, however, infer the existence of a series of sediment-filled rift-valley sequences around and through the plateaux from the Early Cretaceous. Henderson (1980) and Smart and Senior (1980) also drew attention to the necessity of having a felsic-intermediate volcanic zone of considerable magnitude as provenance to Cretaceous sediments in the Great

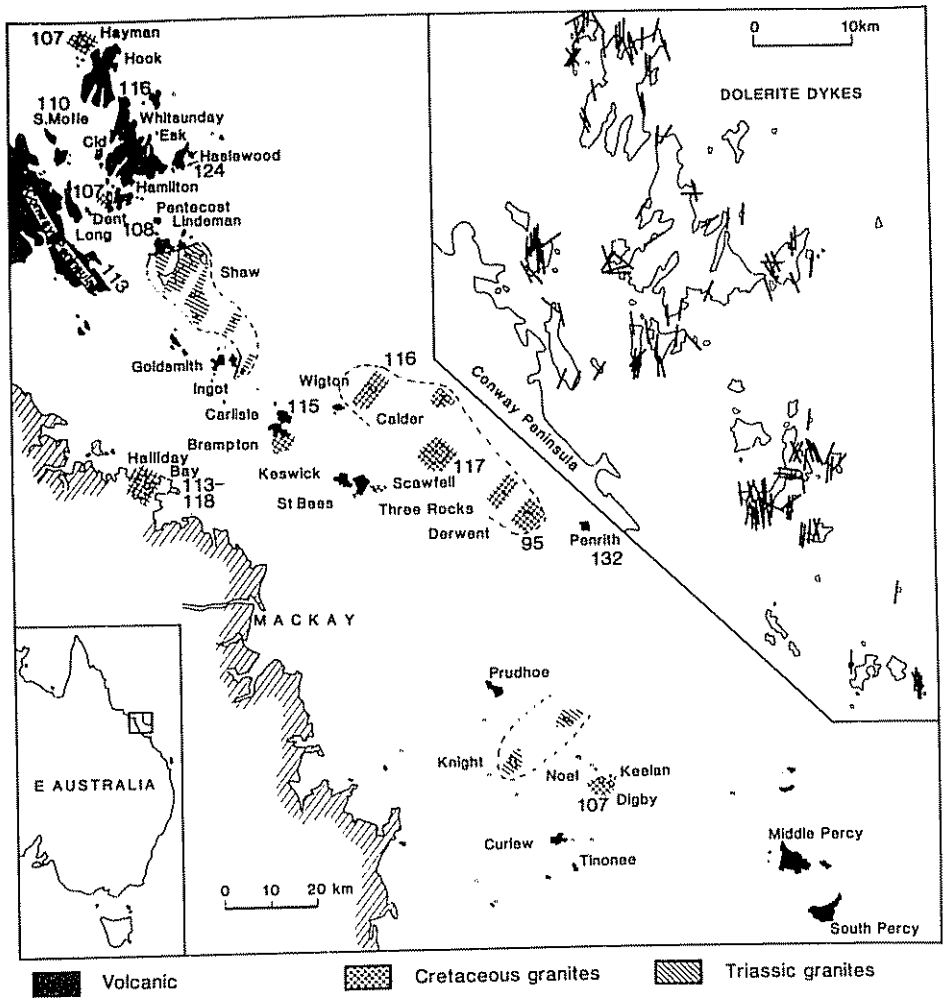

Figure 1 Generalised location map of the central Queensland coast showing the distribution of the Cretaceous volcanics (black) and the Triassic and Cretaceous granites; inset shows the generalised distribution of dolerite dykes in the northern islands; figures are K–Ar and Rb–Sr dates (Table 1) for lavas, ignimbrites, and granites; location of islands referred to in text is shown

Artesian Basin. They infer the site of volcanism to be largely eroded and downfaulted on the present continental shelf, only a small fraction of which is preserved in the Whitsunday and Proserpine volcanics

A divergence of interpretation, however, concerns the tectonic affiliation of the Cretaceous volcanics Veevers (1984, e.g. pp. 136, 137, 205; see also Henderson 1980) consider the volcanics to be part of a magmatic arc associated with a convergent plate boundary which existed several hundred kilometres E of the present eastern Australian coast (see also Veevers *et al.* 1991) The reasoning seems to be based on the petrographically-determined calc-alkaline affinities of the volcanism, and thus the inferred correlation with modern convergent plate margin volcanism.

Other authors, however, clearly identify the Cretaceous eastern Australian margin as a passive divergent margin (e.g. Falvey & Middleton 1981; Falvey & Mutter 1981; Symonds *et al.* 1984, 1988; Symonds & Willcox 1989), with a detachment model being applied by Etheridge and Lister (1987) and Lister *et al.* (1988) to the margins of the Tasman Sea. These models imply no prior convergent phase in the late Jurassic–Early Cretaceous, and the Whitsunday Volcanics are interpreted as erupting within Lower Cretaceous rift basins or troughs developed prior to the actual rifting stage; in fact, it is possible that they occupy early failed rift systems. Falvey and Middleton (1981) suggest that basin subsidence may occur as rift grabens and half grabens flanking incipient continent–ocean boundary as much as 50 Ma before breakup; volcanism is noted to occur only close to the incipient boundary.

In conclusion, therefore, we see no compelling tectonic evidence for the existence of a convergent plate boundary association with the Whitsunday Volcanics. This is considered a significant aspect in the interpretation of the petrogenesis of the magmas.

2. Geochronology

Webb and McDougall (1968) established the Lower Cretaceous ages of the Whitsunday and Proserpine volcanics by means of an eight-point Rb–Sr isochron of 113 ± 5 Ma (corrected from 111 Ma using updated constants) for the Proserpine volcanics, plus four K–Ar dates. This is now supplemented by an additional nine K–Ar dates and 49 Rb–Sr data sets (Table 2) specifically on the Whitsunday Volcanics, and an additional 15 Rb–Sr data sets for the Proserpine Volcanics. The latter provide an identical isochron of 113 Ma to that noted above. A summary of dates is presented in Table 1.

Combined K–Ar and Rb–Sr data on the granites show the existence of both Triassic and Cretaceous granites. The Rb–Sr isochron of the former gives an age of 229 ± 1·1 Ma (MSWD = 2·8), with initial $^{87}Sr/^{86}Sr$ of 0·70353 ± 0·00007. These granites comprise the Shaw Is. and Knight Is. groups, and the ages are confirmed by a K–Ar date from Knight Is.

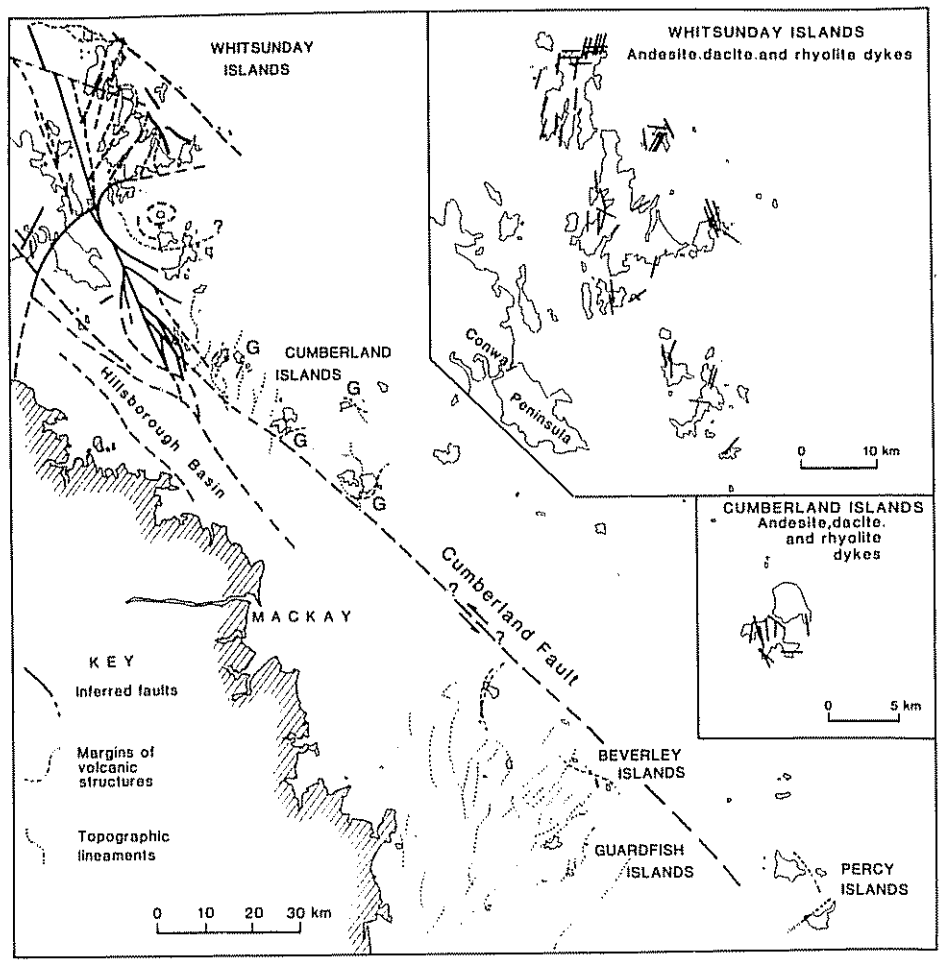

Figure 2 Map of the Whitsunday Volcanics and associated granites, showing inferred fault structures, submarine topographic lineament patterns and volcanic boundaries (the symbol G being used to indicate Cretaceous granite contacts); inset shows the generalised distribution of intermediate to silicic dykes in the northern and central island groups

of 232 ± 3 Ma. The combined data for the Cretaceous granites indicate three discrete age groupings, namely: (i) Scawfell–Three Rocks (K–Ar 116·6 Ma), and the separate Wigton–Calder Is. (K–Ar 116·1, assumed to also apply to Calder Is.) groups; (ii) Derwent Is. (K–Ar 94·8); (iii) the Hayman–Dent–Noel Is. zone which define a single isochron of 107 ± 2·5 Ma. Field relationships show the Dent, Hayman and Noel-Digby granites to be intrusive into volcanics, whereas dolerite dykes are recorded as cutting all but the Derwent granite. The remaining granites have no volcanic contacts exposed.

The age range of the Cretaceous granites suggests that volcanics should also exhibit comparable age ranges. This is certainly confirmed (Table 1), although complicated by apparently varying age patterns between the ignimbrites, lavas and dykes. The ignimbrites define two, and possibly four age groupings, namely 132 Ma (the outlaying Penrith Is.), and 115–117 Ma (the Hook–Whitsunday–Carlisle–Pentecost–Goldsmith Is. group). A possible age grouping of approximately 125 Ma needs further confirmation for the ignimbrites on islands occurring E of Whitsunday Is. (and also E of a major tectonic, possibly collapse structure, Fig. 2), while a younger K–Ar age of 98 and 108 Ma is reported for alunite altered sample from Pentecost (Webb & McDougall 1968), the exact significance of which is uncertain; it is noted, however, that this ignimbrite possesses a distinctive mineralogy, and possibly represents a younger eruptive phase.

The rhyolitic to andesitic lavas post-date the ignimbrites, consistent with field relations, with Rb–Sr ages of 105, 110 and 113 Ma, the youngest group interestingly belonging to the southernmost group of islands. Only three K–Ar dyke ages are available, ranging from 128 Ma on Penrith Is. (containing the oldest ignimbrites), to 107 and 100 Ma. Dyke emplacement thus apparently occurred over an extended time interval, largely coeval with volcanism and granite emplacement. This is consistent with Rb–Sr dyke data which fail to give a geologically meaningful isochron (nominally 126 Ma).

Although still incomplete, the data do suggest a systematic age pattern (Fig. 1), with ages broadly increasing towards the E for the granites and ignimbrites. This pattern tends to reverse on the adjacent mainland for granite emplacement (coeval volcanics being absent). Moreover, within any one zone in the volcanic belt, granite emplacement appears to postdate associated volcanism by up to 8 Ma. In terms of the

Table 1 Summary of radiometric dating on Whitsunday and related islands

	Rb–Sr	K–Ar
1	*Granites*	
	Basement (Shaw Is. group, Knight Is., Conway Peninsula) 229 ± 1·1 (MSWD 2·8)	Knight Is. 232 ± 3 (M)
	Hayman–Dent–Noel 107 ± 2·5 (MSWD 0·1)	Scawfell 116·6 ± 1·3 (H) Wigton 116·1 ± 1·3(H) Derwent 94·8 ± 1·1(H)
2	*Ignimbrites*	
	Hook–Carlisle–Goldsmith–Pentecost 116·5 ± 2·2 (MSWD 1·4)	Penrith 131·8 ± 1·5 (H) Esk 125 ± 3 (H) Carlisle 115 ± 3 (H) Whitsunday 115 ± 2·5 (H) Pentecost 98 and 108 ± 3 (Alunite)
	Esk–Haslewood ~ 124 (2 points)	
3	*Lavas*	
	Shaw–Lindeman–Cid–Hamilton–Ingot 113·3 ± 1·2 (MSWD 1·8)	
	S Molle–Long 110 ± 0·9 (MSWD 1·6)	
	Tinonee–Curlew–Keelan–Keswick 105·4 ± 1·7 (MSWD 1·7)	
4	*Dykes*	
		Penrith (Hornblende andesite) 128·4 ± 1·4 (H) Lindeman (Dacite) 100 ± 3 (H) S Molle (gabbro/dolerite) 107 ± 2 (P)
5	*Mainland*	
	Conway Peninsula 113 ± 3 (MSWD 12·5, 23 points)	Halliday Bay 113 and 118 ± 3 (H) (Separate granite phases)

Date sources: Clarke *et al.* 1971; Webb & McDougall 1968; Ewart & Schon, unpublished data. H = hornblende; P = plagioclase; M = muscovite

Table 2 Frequency % occurrence of phenocryst phases in Whitsunday volcanics, compared to modern southwestern Pacific rhyolite and dacite occurrences

	Rhyolites and dacites Whitsunday Is.	Southwestern Pacific dacites*	Rhyolites of Taupo Volcanic Zone (New Zealand)*
Plagioclase	94	100	97
Quartz	15	14	62
Augite	82	89	9
± Augite + Hypersthene	(82)++	82	94
Hornblende	15+	32	58
Biotite	8+	14	30
Samples	279	141	77

Notes: * After Ewart 1979; + Includes identifiable pseudomorphs after these phases; ++ Hypersthene is altered throughout these volcanics, but is inferred to have been an originally common phase, based on pseudomorphs

rifting model, the age patterns can be interpreted in terms of progressive rifting and volcanism above a linear heat source approximately coincident with the present central Queensland coastline, with net eastward movement of the rifted crustal blocks. The oldest date of 132 Ma (Penrith Is.) is consistent with the lower Cretaceous age of the more southerly Grahams Creek Formation (136 Ma), and ages of 136–145 Ma for associated intrusives (Green & Webb 1974; see also Fig. 18). The total age range for intrusive and extrusive activity is 37 Ma (95–132 Ma) for the Whitsunday region.

3. Outline of volcanic geology

The volcanics are dominated by rhyolitic to dacitic ignimbritic units (ranging from 10–100 m in thickness) throughout the volcanic zone, accompanied by surge and bedded tuff deposits, lenticulitic and pumiceous zones and, on most islands, containing lithic concentration zones and more locally, coarse lag deposits. In fact, a characteristic feature of the ignimbrites is their lithic-rich nature, the fragments comprising volcanic types ranging from andesite and basalt through to fluidal rhyolites, inferred to include Cretaceous and Triassic basement volcanics. In addition to the primary pyroclastics, local thick sequences of phreatomagmatic deposits, and high energy coarse volcanic sandstones are encountered. Lavas are mainly rhyolitic with minor andesites and dacites, and rarely basalts, occurring as isolated flows, lava domes, and basaltic scoria cones.

Dykes are common and characteristic throughout the region, ranging from dolerites to rhyolites, with widths from 0·5–100 m. The dolerites are most abundant in the northern part of the region (Fig. 1), being particularly conspicuous as swarms cutting the granites, and the volanics at the northern end of Hook Is.; there are also some particularly thick (up to 100 m) gabbroic dyke/sill complexes on S Molle Is. This latter locality is especially significant as the geochemically most "primitive" dykes are here. The intermediate to silicic dykes are likewise widespread, locally up to 40 m thick (these thicker units inferred to be volcanic feeders), the most intense concentration occurring again at the northern end of Hook Is. (Fig. 2). Dyke trends are dominantly northerly for all types, with only local northwesterly and southwesterly trends developed. Dolerites are noted to cut rhyolitic dykes in the rare dyke intersections observed.

3.1. Volcanic environments

The volcanic sequences are interpreted as subaerially deposited, with only localised shallow water deposits (cf. Clarke *et al.* 1971). The deposits within the majority of islands are interpreted as "intracaldera" facies. Supporting evidence includes: (i) Estimated thicknesses of >1 km for the sequences on at least Hook, Whitsunday, and Lindeman Is; the occurrence of massive ignimbritic units on other islands likewise indicates total thicknesses greater than typical of outflow facies; (ii) pervasive low grade hydrothermal alteration; (iii) the abundance of intermediate to silicic dykes; dolerites seem most abundant either in the granites, or close to inferred caldera collapse margins; (iv) occurrences of very coarse lag deposits, some with clasts 3–6 m in diameter.

Figure 2 shows the inferred distribution of the tectonic boundaries and structures, based on limited available aeromagnetic data, with other structural lineaments from bathymetry, exposed basement-volcanic contact zones and the distribution of inferred near-vent pyroclastic facies. One major boundary lies along the eastern margin of Hook and Whitsunday Is., swings westward to the northern end of Hayman Is., with the southern margin passing through the Shaw–Lindeman Is. groups (Figs 1, 2); this boundary is believed to represent a volanic-collapse feature. The islands E of Whitsunday tend to preserve less-altered pyroclastics and are inferred to represent (older) outflow facies. This structure is the only "caldera-like" collapse structure so far recognised in the region, the southern volcanic centres being far more fragmented, and perhaps graben-controlled.

The overall regional pattern of volcanicity is thus interpreted as involving multiple vent eruptions, localised within at least four centres of collapse, and aligned along a complex volcano-tectonic rift depression, possibly of the style seen in the Taupo Volcanic Zone of New Zealand, although with much greater length.

4. Petrography

4.1. Volcanics

4.1.1. Rhyolites and dacites. Based on phenocryst assemblages, the following mineralogical groups are recognised:

(i) Plagioclase, augite, Ti-magnetite, ± uralitised orthopyroxene. This is the predominent mineralogical assemblage throughout the region. Phenocryst abundances range from <5% (commonly <2%) in lavas, to typically between 5–15% (with local crystal-rich lithologies) occurring within ignimbrites (eruptive crystal concentrations).

(ii) Plagioclase, quartz, augite, and Fe–Ti oxides, with 5–20% total phenocrysts. This assemblage is found within some ignimbrites of the central and southern islands, but is generally uncommon.

(iii) Plagioclase, augite, hornblende, and Fe–Ti oxides, with phenocryst abundances ranging from 5–25%, and rarely containing biotite. This assemblage occurs in dykes and commonly in ignimbrites from Hook, Esk, and Haslewood Is. within the northern area, and Penrith and Middle Percy in the southern area.

(iv) Plagioclase, quartz, hornblende, augite, and Fe–Ti oxides, with phenocryst contents 15–30%. This assemblage occurs rarely in dykes, being most characteristic of the Carlisle and some Long Is. ignimbrites.

(v) Plagioclase, quartz, biotite, augite, and Fe–Ti oxides, with phenocryst contents of 10–30%. This is found within dykes and the Pentecost Is. ignimbrites.

(vi) Plagioclase, sanidine, quartz, biotite, ± hornblende, Fe–Ti oxides; phenocryst contents 20–40%. This occurs in some dykes, and very rarely in high-silica rhyolitic ignimbrites.

4.1.2. Andesites, basalts and dolerites. Dolerite dykes and the rare basalts are usually nearly aphyric, with sparse augite and/or plagioclase phenocrysts. Andesite dykes and lavas characteristically contain phenocrystal plagioclase (15–30%), augite (3–10%), uralitised orthopyroxene (3–5%), and Ti-magnetite.

4.1.3. Discussion. Only relatively rare extrusive equivalents of the dolerite dykes are found, most notably as local basalt flows on S Molle and Lindeman Is. Dykes, plugs, and flows of andesite, however, occur sporadically throughout the region. The rhyolitic lavas with very low phenocryst abundances have no pyroclastic equivalents, although the pyroxene and hornblende-bearing rhyolitic dykes have equivalents among the ignimbrites. The sanidine-bearing rhyolite dykes apparently have only extremely rare ignimbritic equivalents. Relative dyke ages are poorly

constrained, but dykes having assemblages (v) and (vi), above, cut rhyolite domes and an andesite plug, both of the latter inferred as among the youngest extrusive phases. The youngest dyke dated (100 Ma; Table 1), from Lindeman Is., has a type (iv) assemblage.

Comparison of the overall pattern of phenocryst abundances with modern southwestern Pacific "orogenic" silicic volanics (Table 2) shows the closest similarity with the orogenic dacites, but even here, the Whitsunday volanics apparently contain less common hornblende and biotite; they are clearly predominantly pyroxene rhyolites and dacites.

Secondary alteration. Low grade pervasive hydrothermal alteration is a regional characteristic of the volcanics, usually more extensively developed in the pyroclastics, but also occurring as microveining in lavas. Secondary phases include albite, chlorite, calcite, epidote, zoisite, sericite, actinolite, quartz, and sphene, with localised developments of prehnite, pyrite, laumontite, pyrophyllite and alunite.

4.2. Granites

These range from granite (s.s.) to quartz diorite, and petrographically fall into natural groupings:

Derwent. Strongly porphyritic, with phenocrystal K-feldspar + quartz + minor plagioclase + accessary Fe-hornblende, biotite, allanite, magnetite and rutile.

Scawfell and Three Rocks. Perthite + quarz + plagioclase (rimmed by K-feldspar) + accessory hornblende, biotite, allanite, ilmenite + magnetite.

Digby and Noel. Porphyritic, with plagioclase + quartz + perthite (interstitial to, and rims plagioclase) + accessary hornblende (rare augite cores), biotite, sphene, + ilmenite.

Dent. Porphyritic with plagioclase (K-feldspar rims) + quartz + K-feldspar + accessary pyroxene, magnetite, + rutile.

Hayman, Wigton and Calder. These contain abundant but irregularly distributed inclusions, and range from adamellite to granodiorite. They contain plagioclase (K-feldspar rims) + quartz + K-feldspar + accessary hornblende, biotite, sphene, allanite, magnetite, ilmenite, ± rutile. Hayman granites also contain some remarkably euhedral epidotes, suggesting primary crystallisation (although not readily reconciled with their shallow emplacement). The most significant aspect of these granites is the presence of abundant quartz diorite inclusions, locally forming spectacular zones of mingling. The inclusions are veined and injected by granodiorite-adamellite melt, and all stages of disaggregation are present from 20 m-long tabular "rafts" of quartz diorite to small diffuse "clots". The inclusions are fine to medium grained, consisting of plagioclase with interstitial quartz, K-feldspar plus accessory hornblende, ± augite, ± biotite, magnetite and ilmenite.

5. Mineralogy

Plagioclase. Compositions are commonly modified by albitisation, but remnant primary compositions are sufficiently often preserved to determine original compositional ranges. Within the dolerites (including basaltic andesite dykes), plagioclase (mainly coarse groundmass, less often phenocrystal) ranges from labradorite to bytownite, although within the coarse doleritic dyke/sill complexes on S Molle, plagioclases are zoned continuously through to oligoclase, due to *in-situ* fractionation. Phenocrystal andesite plagioclases are labradorite to median bytownite, whereas, in the dacitic ignimbrites, dominant compositions are andesine, although it is common to find individual crystals of labradorite–bytownite compositions. Low-silica rhyolitic dykes and ignimbrites also exhibit divergent plagioclase compositions (labradorite–andesine), suggesting that these are not simply the result of eruptive entrainment of andesitic lithic clasts into ignimbrites, and tend to point to a pre-eruptive mixing process. High-silica rhyolites contain oligoclase, in some examples coexisting with a sodic sanidine phase, but again sporadic isolated more calcic plagioclase occurs.

Pyroxene and amphiboles (Figs. 3, 4). Only calcic pyroxenes are preserved, although orthopyroxene is inferred to have originally been a widespread phase in the andesitic and rholitic volcanics. Reference to the pyroxene compositional ranges shows that with the exception of high silica rhyolites, there is little variation in Fe–Mg–Ca ratios throughout the dolerite to low-silica rhyolite magma compositions. In fact, the general compositions are relatively magnesian, this being a common "orogenic" characteristic, and is emphasised by the overlap of the compositional fields with the respective modern Southwestern Pacific "orogenic" pyroxenes (shown by the circled fields in Fig. 3). Within the doleritic pyroxenes, the more calcic pyroxene (and higher Al and Ti) compositions are found within the *ne*- and *ol*-normative dolerites, indicating that the silica-undersaturated chemistry of these dolerites is a primary magmatic feature. Fe-enriched compositions only occur in the rhyolites, most notably the high-silica types, but significantly, bimodal pyroxene compositions are found in some low and high-silica rhyolites (Fig. 3, h-i). Evidence for mixed pyroxene compositions, most notably in some andesites, a trachyandesite, and dacites, also comes from either bimodal Al solid solution abundances, or wider ranges of Al than normally found in pyroxenes from such rocks. The high-silica rhyolite pyroxenes exhibit very limited Al solid solution ranges.

With the exception of rare Fe-rich hornblendes in high-silica rhyolites, the phenocrystal volcanic hornblendes are consistently relatively magnesian, and are again similar to compositions within "orogenic" silicic volcanics (e.g. Ewart 1982). In terms of major cation substitutions (Fig. 4), the amphiboles range from actinolitic hornblende in the rhyolites through hornblende in the rhyolites and dacites, towards hastingsite in the andesites and some dacites. Relict kaersutite is recorded in a single "mixed" andesite. The total data exhibit a very smooth trend through the compositional range, but as with the pyroxenes, bimodal compositional ranges are observed in dacites and low-silica rhyolitic ignimbrites and dykes. Application of the amphibole–plagioclase geothermometer (Blundy & Holland 1990) has not provided definitive temperature estimates, as taking extremes of compositional ranges found within relevant dacites and low-silica rhyolites gives an exaggerated temperature range between 620–1170°C. This is suggested to reflect disequilibrium among these compositions.

Amphibole compositions in the granites exhibit differences from those in the volcanics (Figs. 3, 4). Firstly, there is a tendency for increasing Fe-enrichment, most pronounced in the late-stage Derwent porphyritic granite. Secondly, the compositions are offset towards more edenitic compositions, especially pronounced in the Derwent hornblendes. Other hornblendes, however, tend toward more actinolitic compositions, and this is attributed to solidus–subsolidus re-equilibration processes.

Fe–Ti oxides. Titaniferous magnetite is the dominant oxide phenocryst phase in the andesites and dacites, in some samples, coexisting with minor ilmenite. Coexisting oxide

phases occur in the rhyolites, often exhibiting marked Mn enrichment. T°C and f_{O_2} estimates from a few available relatively homogeneous compositions suggest rhyolitic equilibration temperatures of 800–900°C, the hornblende-bearing types lying above NNO buffer, and the pyroxene rhyolites between NNO and FMQ.

6. Chemistry

6.1. Major elements

The overall range, and continuity of compositions of the volcanic and intrusive phases is readily apparent from the total alkalis–silica plot (Le Maitre 1989; Fig. 5). The bulk of

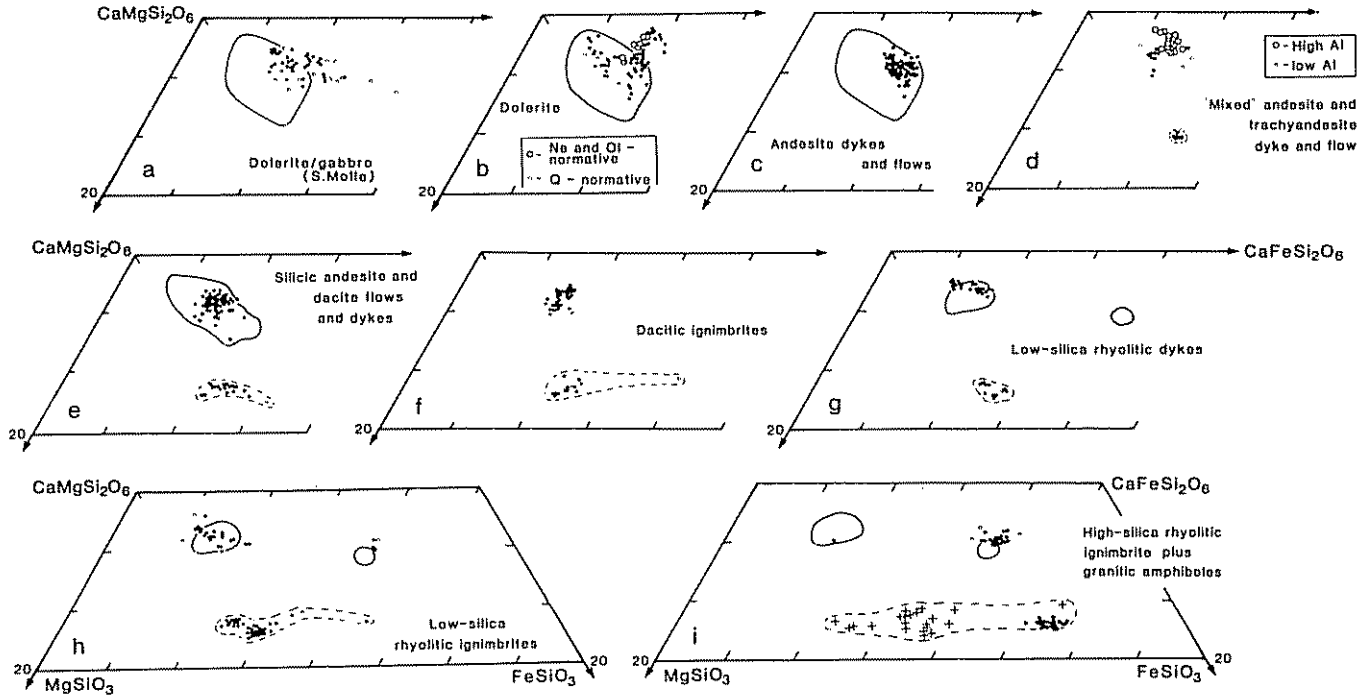

Figure 3 Pyroxene and amphibole phenocryst compositions in the Whitsunday Volcanics and Cretaceous granites ((i) only), expressed in terms of Ca, Mg, and Fe + Mn (atomic %); continuous circled fields are the pyroxene fields from southwestern Pacific "orogenic" lavas of the equivalent bulk rock compositions (after Ewart 1979, 1982); data lying in the dotted fields are amphibole compositions; in (i), the crosses represent granite amphiboles excluding Derwent Is., while the filled black dots represent Derwent Is. amphiboles

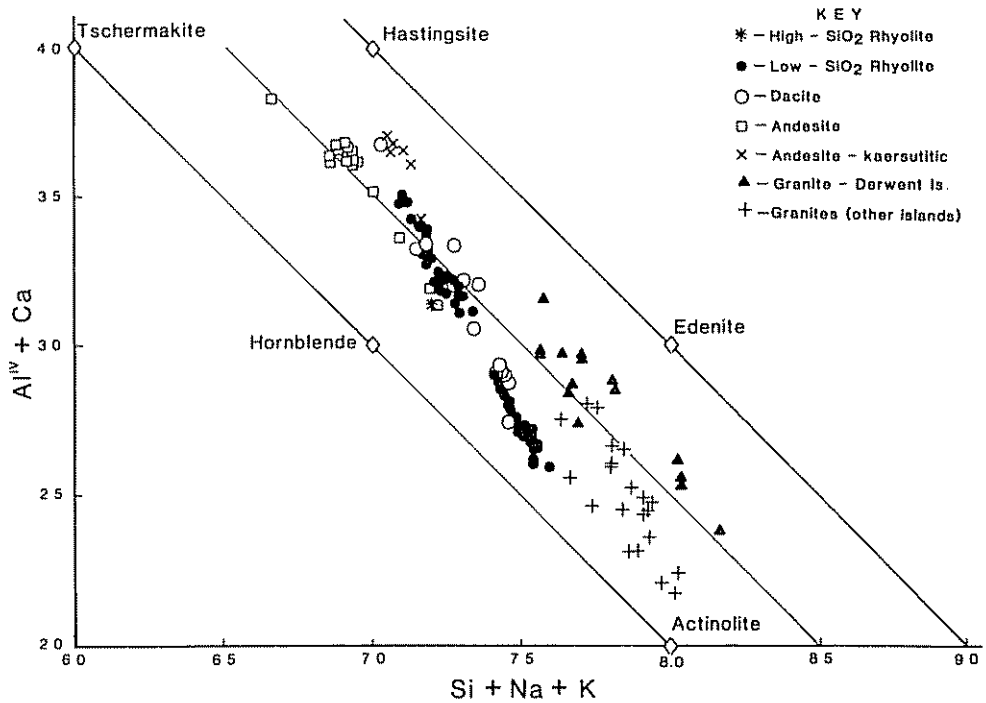

Figure 4 Amphibole phenocryst compositions in the Whitsunday volcanics and coeval granites

the data plot within the basalt–basaltic andesite–andesite–dacite–rhyolite fields, with a relatively small percentage classifying as "alkalic", especially in the trachyandesite field. In this respect, the Cretaceous suite contrasts strongly with the alkaline eastern Australian Cainozoic intraplate provinces (Ewart *et al.* 1988), but is comparable with the overall calc-alkaline chemistry of many modern western Pacific island arc regions (e.g. Ewart 1979, 1982). The rhyolites are almost all peraluminous, averaging 1·2% normative corundum; this compares with 0·8% for the granites.

Figure 6a–d illustrates the silica distribution in relation to modes of occurrence. The ignimbrites and dykes exhibit continuous ranges from dolerites to rhyolites (dykes) and andesite to rhyolite (ignimbrites). The dykes exhibit a relatively constant frequency across the whole silica range

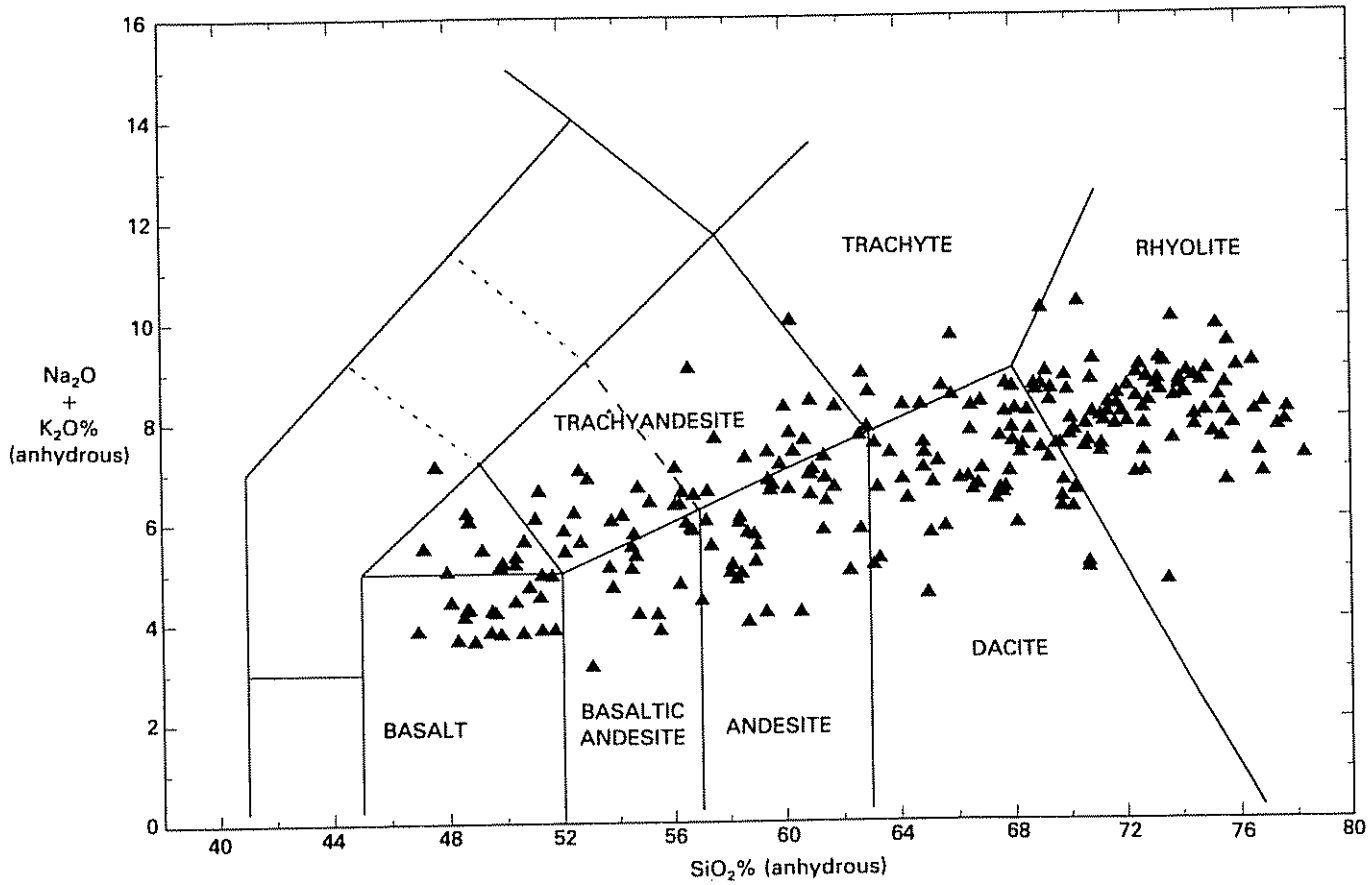

Figure 5 Total alkalis–silica plot of the Whitsunday volcanics and Cretaceous granites; field boundaries are after Le Maitre (1989)

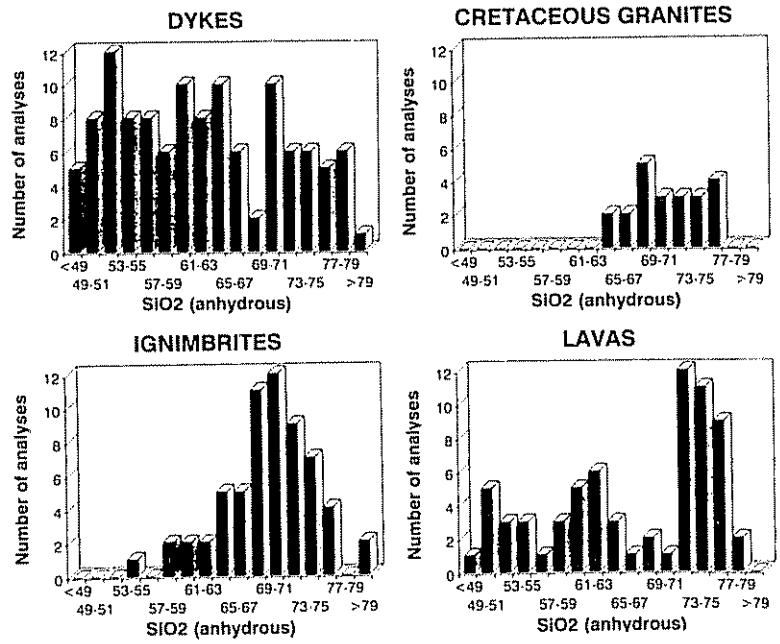

Figure 6 Silica histograms showing the distribution of compositions within the dykes, lavas, and ignimbrite, and coeval granites

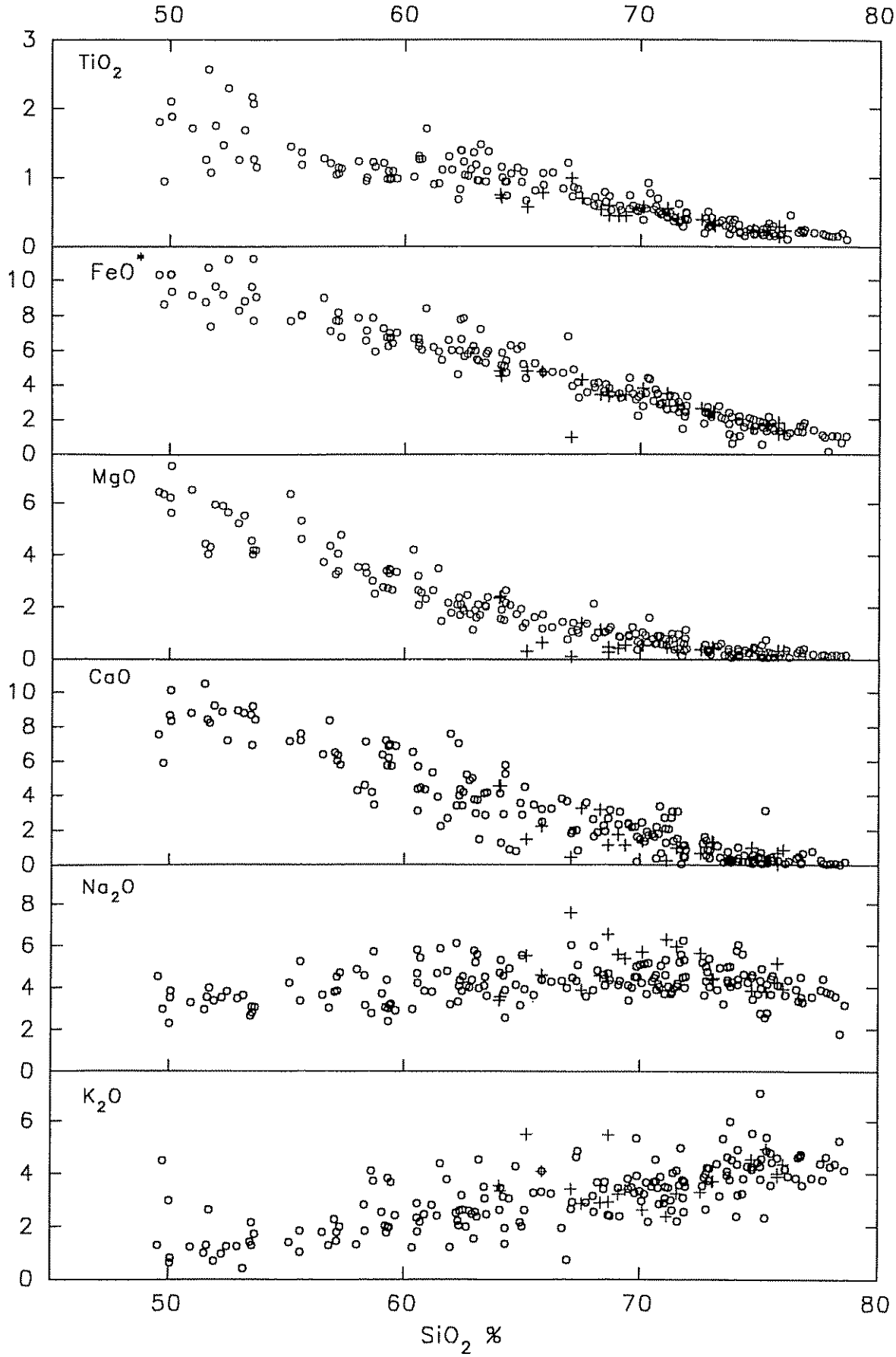

Figure 7 Composite Harker Diagrams for the Whitsunday Volcanics and (crosses) Cretaceous granites

while the ignimbrites are dominantly dacitic to low-silica rhyolites. In contrast, the lavas tend to be trimodal, with distinct basalt, andesite and high silica rhyolite types.

Harker diagrams (Fig. 7a–i) show the expected trends with respect to silica, and are generally comparable to those of the New England granites (Shaw & Flood 1981), although differences exist with respect to MgO, CaO and FeO*. The Whitsunday data exhibit a wider scatter for the alkalis and CaO, possibly reflecting alteration effects. The TiO_2 and P_2O_5 data also exhibit some divergence at the mafic end of the range, almost certainly reflecting a range of doleritic compositions from *ne*- to *Q*-normative. As the majority of mafic dykes are labradorite-normative, they classify as alkali olivine basalts to tholeiites, although the majority are olivine to quartz tholeiites.

In terms of normative Ab-Or-Q components (Fig. 8), the silicic volcanics and granites are of sodic, rather than potassic affinities. The Triassic and Cretaceous granites are compositionally distinct, and with one exception, the former represent hypersolvus minimum-temperature melt granites whose compositions project near the 100 MPa water-saturated piercing point in the $[Ab\text{-}Or\text{-}Q]_{97}An_3$ system (James & Hamilton 1969). The Cretaceous granites, in contrast, extend from near minimum-temperature melt compositions (e.g. Scawfell–Derwent Is. group) to granodiorites, and cluster into distinct groupings usually reflecting similar chemistry between geographically closely-spaced islands. The trends of the data fields vary, with some apparently controlled by a four-phase surface as defined in the Ab-An-Or-Q-H_2O system (Nekvasil 1988), while other granite data fields are cross-cutting, possibly representing dioritic mixing trends (i.e. the inclusion-rich granites, previously noted).

The rhyolitic volcanics (Fig. 8a–c) define similar compositional fields to the coeval granites, although with variable trends. The high-silica rhyolites project closest to the minimum-temperature compositions, although phenocrystal quartz and sanidine are uncommon. In the plots, however, the quartz-bearing dykes and ignimbrites are distinguished, and are seen to define distinct fields. Considered overall, the rhyolitic compositions are consistent with magmas evolving under relatively low (<200 MPa) pressures. One possible exception is the group of phenocrystal quartz-bearing, low-silica rhyolitic to dacitic ignimbrites (Carlisle and Long Is.) which appear to have equilibrated at higher pressures. The mineralogically distinctive Pentecost Is. ignimbrites (plag–qtz–biot–augite) also define a unique compositional field, although the higher normative Q portion is alteration controlled. Apart from these exceptions, the bulk of the rhyolitic data for the dykes, lavas, and ignimbrites exhibit completely overlapping compositional groupings, and unlike the granites, cannot be divided into distinctive island groupings (i.e. volcanic centres).

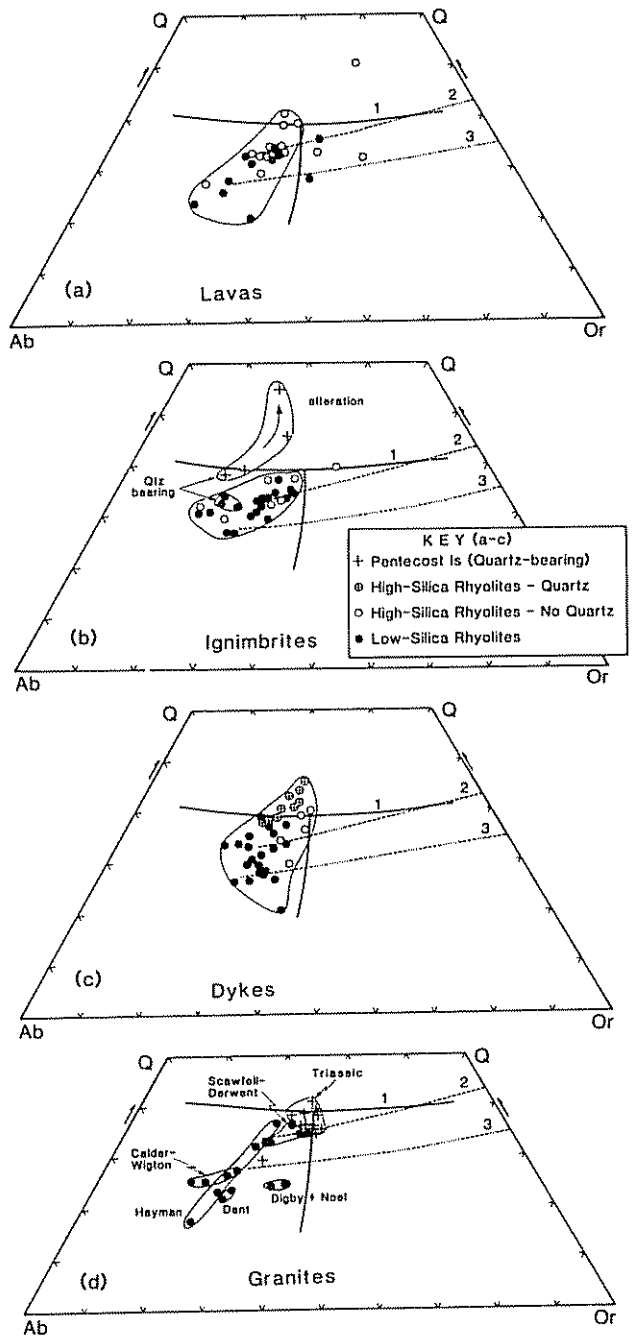

Figure 8 Normative Q–Ab–Or components of the rhyolite lavas, ignimbrites, and dykes, and the granites; boundary curves are: 1, water saturated curves, 100 MPa for composition An_3 after James and Hamilton (1969); curves 2 and 3 are the calculated 4-phase surfaces in the system Ab–An–Or–Q–H_2O for $a_{H_2O} = 1.0$ and 0.2 respectively, at 200 MPa (after Nakvasil 1988); in (a) to (c), the main groups of data are circled, excluding outlying points believed to be modified by alteration.

6.2. Trace elements

6.2.1. Introduction. Data are based on XRF and neutron activation analyses, and representative data are presented in Table 3. In terms of general element behaviour, Rb and Th are incompatible throughout the compositional range, whereas Ba and Zr exhibit similar behaviour only up to the high-silica rhyolite range, indicating late stage control by feldspar and zircon fractionation, respectively. W, Ta, and LREE are broadly incompatible, whereas Nb and Y exhibit little systematic variation throughout the whole compositional range. Elements such as Sc, V, Ni, and Cr correlate with FeO* and MgO, behaving compatibly. The important overall point shown by the trace element data is again the continuity of element abundance patterns.

Mineralogical evidence suggests the possibility of mixing as an important process in these magmas. Routine plotting of many element ratio combinations has shown a number that apparently follow mixing trends, although not all can be easily distinguished from fractional crystallisation trends. One example is illustrated (Fig. 9), for Yb/Th–Ce/Th. Both sets of data (<69% and >69% SiO_2) lie along a linear mixing curve, and the insets show attempts at modelling the variation in terms of fractional crystallisation. These

calculated curves, utilising basaltic andesite, granodiorite, and low-silica rhyolite starting compositions, suggest that neither the trends, nor more importantly, the extents of fractionation, match the observed data trends. It is noted here that attempts to model the overall trace element variations of the whole volcanic suite, using fractional crystallisation and AFC models, have generally been unsuccessful, even though satisfactory major element fits can be established by least squares method for fractional crystallisation only models. As will be further shown, mixing

Table 3 Selected chemical analyses of Whitsunday volcanics and granites

	SM11	Li06	Pr01	Es01	Hs17	No02	Sc04
SiO_2	50·07	59·38	60·6	69·12	74·10	64·08	74·68
TiO_2	1·87	0·97	1·25	0·59	0·21	0·75	0·24
Al_2O_3	17·51	16·81	17·20	15·76	13·55	16·22	13·71
Fe_2O_3	1·58	1·13	1·08	0·58	0·37	0·81	0·25
FeO	7·89	5·66	5·41	2·91	1·83	4·04	1·25
MnO	0·18	0·14	0·14	0·11	0·08	0·08	0·05
MgO	7·46	3·14	2·09	0·87	0·30	2·37	0·33
CaO	8·36	6·98	5·68	2·32	1·00	4·54	0·98
Na_2O	3·81	3·15	4·19	4·11	4·12	3·37	3·85
K_2O	0·81	1·98	1·80	3·46	4·38	3·53	4·54
P_2O_5	0·46	0·37	0·56	0·16	0·07	0·21	0·11
LOI	(2·89)	(2·66)	(2·77)	(3·15)	(2·42)	(2·37)	(2·37)
Rb	20	60	47	97	134	115	143
Cs	1·4	2·0	1·4	3·5	2·6	3·1	4·6
Ba	197	416	393	566	710	365	449
Sr	551	539	610	336	121	435	125
Zr	199	167	231	278	319	218	130
Hf	3·7	3·9	5·2	6·5	7·8	6·6	3·8
Y	31	25	34	36	44	23	24
Ta	0·73	1·4	1·2	1·5	2·0	2·3	1·7
Nb	11	8	10	10	11	6	9
Zn	109	92	99	93	77	78	42
Cu	66	30	23	17	8	41	5
Ni	109	14	15	22	1	68	17
Cr	289	50	8	13	7	56	11
V	183	172	132	38	9	131	13
Sc	25·6	22·0	18	12	9·1	14	3·1
Th	0·5	6·8	5·6	9·1	13·0	19·0	17·5
La	14·2	20·0	27·0	27·0	33·0	25·5	25·5
Ce	36·7	48·0	66	65	79	62	53
Nd	23·6	26·7	39·0	35·5	42·0	32·5	21·5
Sm	5·6	5·5	8·3	7·2	8·5	6·1	3·5
Eu	1·89	1·48	2·20	1·78	1·44	1·23	0·58
Gd	6·3	5·0	7·5	6·3	7·6	4·9	3·0
Tb	0·92	0·88	1·15	1·10	1·30	1·00	0·65
Ho	1·14	0·92	1·45	1·45	1·70	1·05	0·75
Yb	2·95	2·58	3·45	3·65	4·45	2·45	1·90
Lu	0·45	0·39	0·52	0·57	0·68	0·37	0·29

Samples

SM11—Dolerite dyke/sill (100 m thick), S Molle Is.
Li06—andesite lava, Lindeman Is.
Pr01—Andesite dyke, Prudhoe Is
Es01—Ignimbrite, Esk Is.
Hs17—Ignimbrite, Haslewood Is.
No02—Granodiorite, Noel Is.
Sc04—Granite, Scawfell Is.

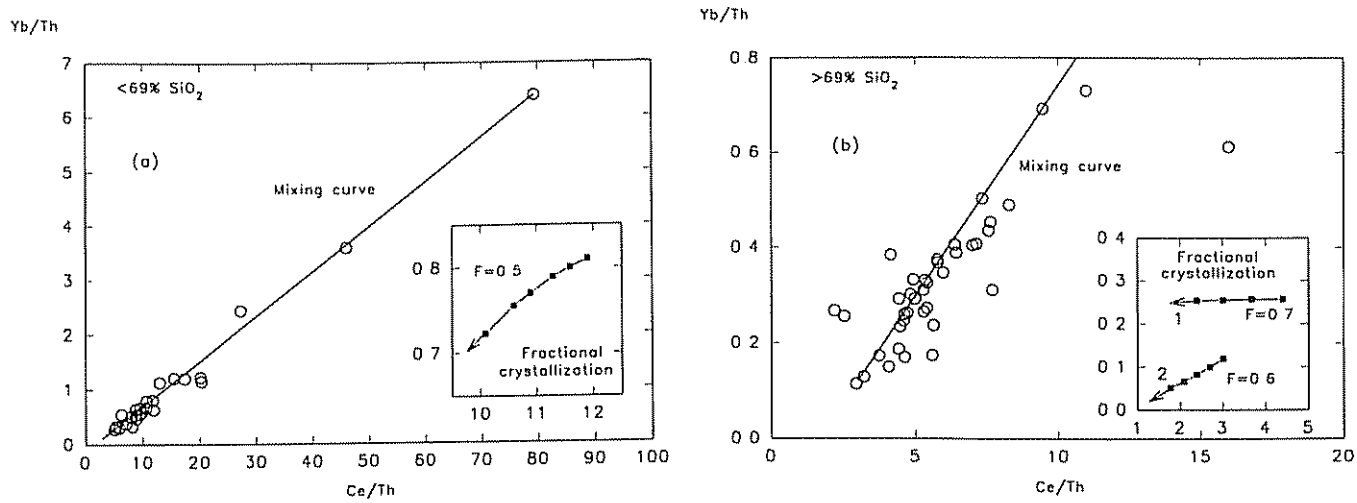

Figure 9 Yb/Th–Ce/Th plot for the Whitsunday volcanics and granites, divided into <69 and >69% SiO_2 groupings; inset in (a) represents the calculated fractional crystallisation curve for a basaltic andesite to granodiorite (dacite), extending to $F = 0·5$ (Plag 0·59, Cpx 0·12, Opx 0·20, Mag 0·06, Ilm 0·02, Ap 0·01); inset in (b) represents calculated fractional crystallisation curves from granodiorite to low-silica rhyolite (Curve 2; Plag 0·63, Cpx 0·16, Opx 0·14, Mag 0·02, Ilm 0·03, Ap 0·02) and low-silica to high-silica rhyolite (Curve 1; Plag 0·83, Cpx 0·07, Mag 0·10)

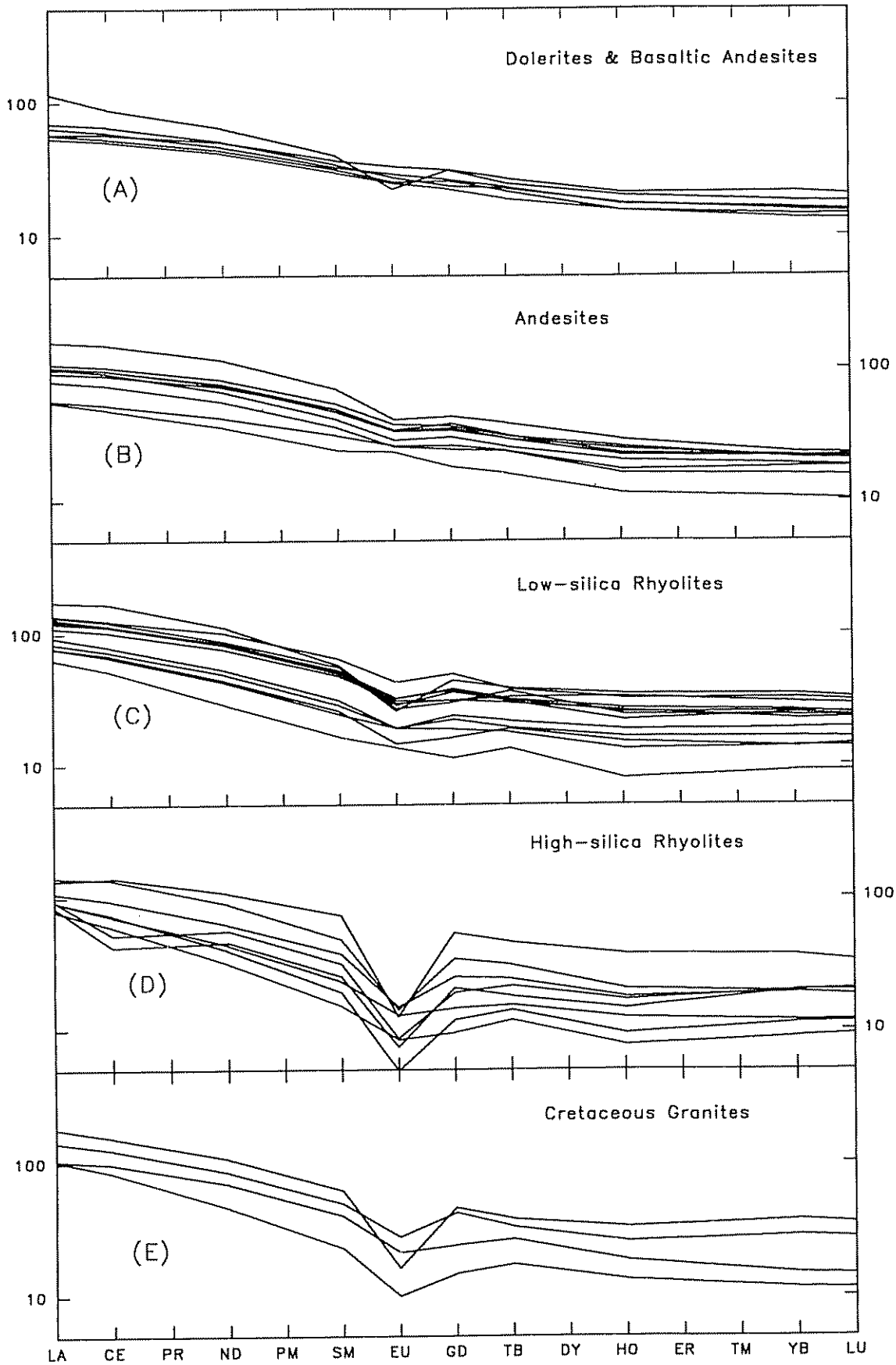

Figure 10 Chondrite-normalised REE abundances comparing the major bulk rock volcanic groupings, and the Cretaceous granites.

relationships have proved the most successful, although superimposed fractional crystallisation has certainly occurred.

6.2.2. Rare earth elements. Selected patterns are illustrated in Figure 10, for the major bulk rock volcanic groupings and granites. The overall data indicate that: (i) the dolerites, basaltic andesites, and andesites exhibit similar patterns, with La_N/Yb_N ratios between 3·2–5·4 (one sample 6·7), the majority between 4·0–5·4. A positive correlation is apparent between La_N and La_N/Yb_N, while very small negative Eu anomalies are present in a few patterns; (ii) the rhyolite patterns entirely overlap those of the andesites, with generally slightly higher LREE compared to dolerites and basaltic andesites. La_N/Yb_N ratios lie between 3·6–6·0, with the highest ratio extending to 8·9. The rhyolites are thus not strongly fractionated in terms of their REE abundances or LREE fractionation. Negative Eu anomalies are most strongly developed in the higher-silica rhyolites; (iii) the Cretaceous granites are intermediate between the low- and high-silica rhyolites.

As the Eu anomalies are indicative of feldspar fractionation, it is relevant to relate Eu/Eu* with Ba and Sr abundances (Fig. 11a, b). The Sr abundances show a systematic decrease with increasing Eu depletion, explicable in terms of plagioclase-dominated fractionation. Ba-Eu/Ea* relations are more complex, showing initially increasing Ba with decreasing Eu/Eu*, followed by limited Ba depletion with further Eu depletion (i.e. at Eu/Eu* < 0·6). This again is consistent with feldspar fractionation, allowing for the changing value of K_D within increasingly siliceous magmas, but the more extreme late state Ba depletion seems to require the presence of sanidine in the fractionating assemblage in the high-silica rhyolites, a phase not commonly observed. Calculated mixing curves (not shown) do not duplicate these observed data trends.

7. Tectonomagmatic affinities

The association of dolerites, through andesites and rhyolites, and coeval granites, is a common association in modern subduction-related volcanic provinces (e.g. Ewart 1982). As previously discussed, however, the Whitsunday volcanics appear more feasibly related to rifting and crustal thinning, rather than a convergent tectonic environment.

The existence of a possible subduction-signature is explored in Figures 12–14. The Ba/Nb–La/Nb data (Fig. 12a, b) show a complete gradation from "intraplate" (as exemplified by the eastern Australian Cainozoic provinces), to arc-like (as exemplified by the Southwestern Pacific

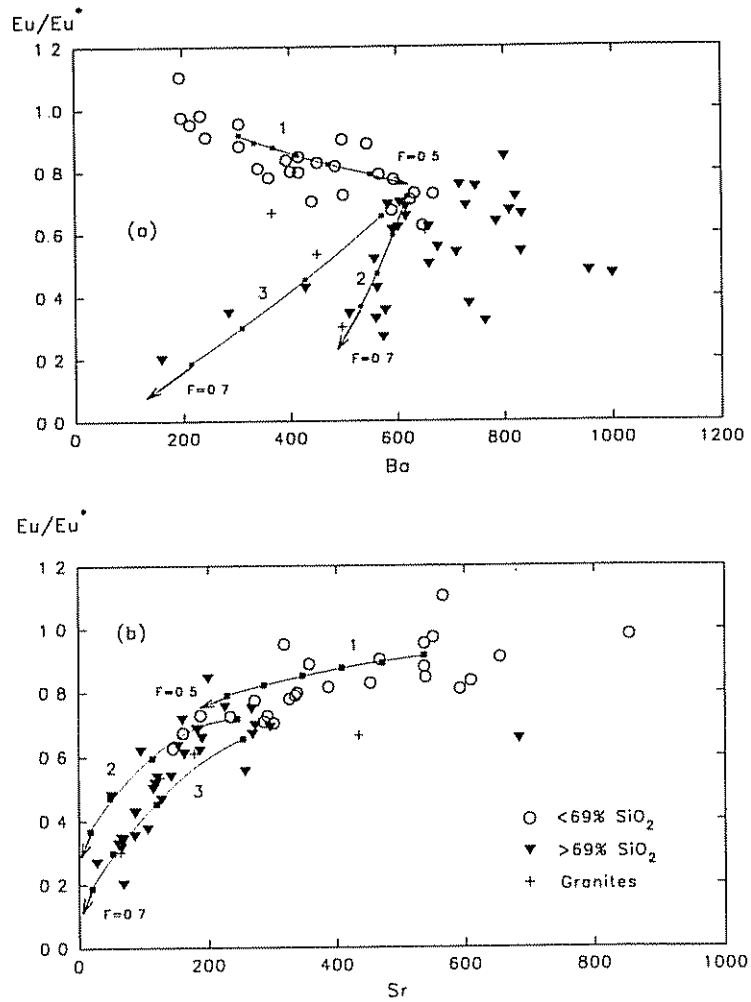

Figure 11 Eu anomalies versus Ba and Sr (ppm), the data divided into <69 and >69% SiO_2, and granite groupings; calculated fractional crystallisation paths are shown for: 1, basaltic andesite to granodiorite (dacite; Plag 0·59, Cpx 0·12, Opx 0·20, Mag 0·06, Ilm 0·02, Ap 0·01); 2 and 3, low-silica rhyolite (two different starting compositions) to high-silica rhyolite; curve 3 incorporates sanidine into the fractionating assemblage (Plag 0·83, Cpx 0·07, Mag 0·10 and Plag 0·60, San 0·32, Cpx 0·01, Mag 0·07, respectively); high-silica rhyolite partition coefficients used in curves 2 and 3.

andesites, and the Taupo Volcanic Zone rhyolites). In fact, the Whitsunday data appear to be in part transitional. The data trends are not readily explained in terms of fractional crystallisation, especially as the fields for the lower silica (<69% SiO_2) and higher silica volcanics and granites almost completely coincide. This suggests that these somewhat variable and transitional geochemical characteristics are source related. Significantly, many of the dolerites plot within the eastern Australian Cainozoic intra-plate fields.

Further comparisons between possible arc-like and within-plate signatures for the Whitsunday volcanics and granites are presented in terms of the ternary Hf–Th–Ta abundances (after Wood 1980; Fig. 13) and Th/Yb–Ta/Yb ratios (after Pearce 1983; Fig. 14). In Figure 13, the data plot as a remarkably linear array which is most readily explicable as a mixing array, as shown by the calculated mixing lines. Fractional crystallisation certainly cannot give rise to such an array. The mafic end of the spectrum is also informative, projecting in the E-type MORB and within-plate tholeiitic fields, whereas the silicic volcanics and granites plot predominantly within the calc-alkaline "destructive margin" volcanic field.

Further confirmation of the previous data trends is obtained in Figure 14, the data again defining an array consistent with a two-component mixing process. One end of the array, defined by dolerite and basaltic andesite dykes, lies in the mantle array (near average E-type MORB), whereas the main body of the data lie in the region defined by Pearce (1983) as characterising calc-alkaline to shoshonitic active continental margins, and alkaline oceanic

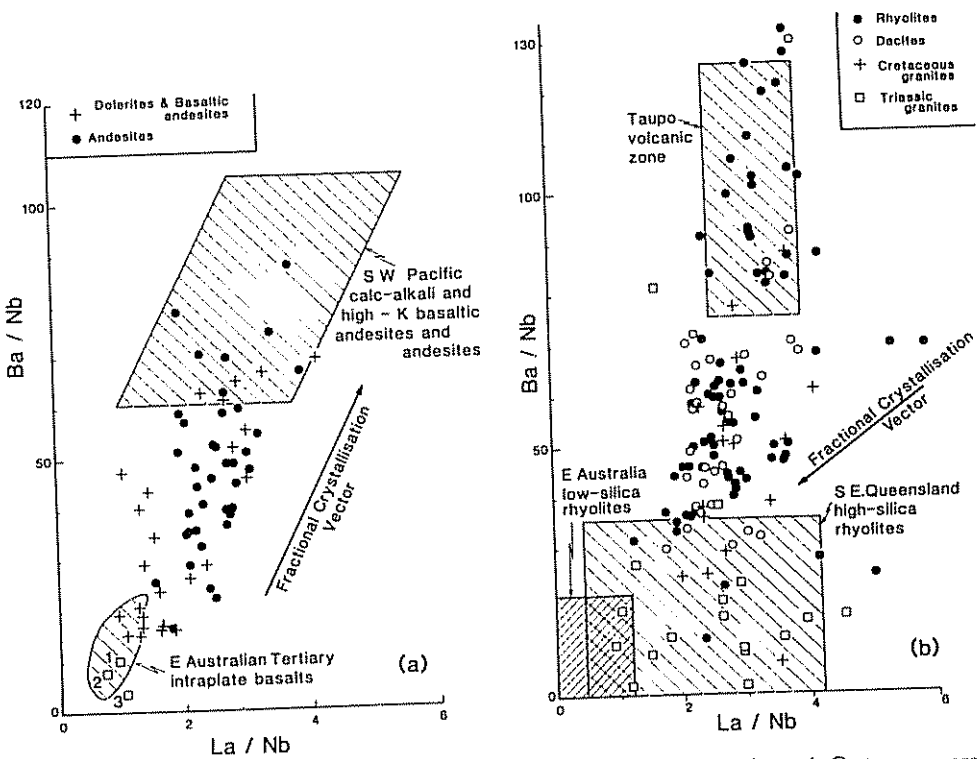

Figure 12 Ba/Nb–La/Nb plots for the Whitsunday Volcanics and Triassic and Cretaceous granites; intraplate fields are after Ewart and Chappell (1989), the averaged southwestern Pacific andesites after Ewart (1982), and the Taupo Volcanic Zone rhyolites after G. Corlett (pers. comm.); hollow squares labelled 1, 2, and 3 in (a) are the average primitive mantle, E-type MORB, and N-type MORB, respectively (after Sun and McDonough 1989).

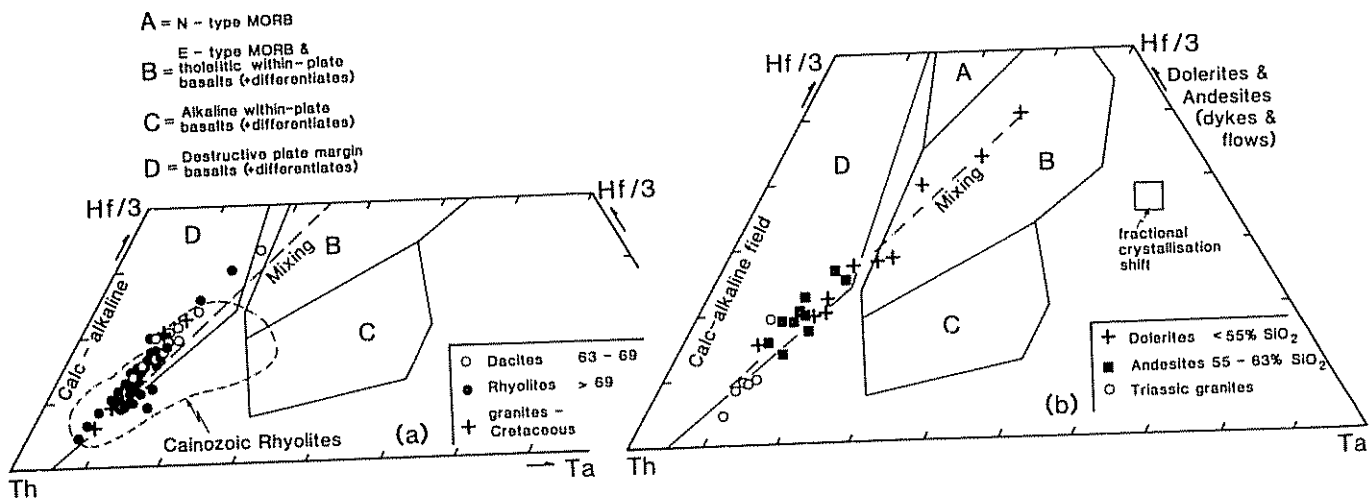

Figure 13 Hf–Ta–Th relationships of the rhyolites, dacites and Cretaceous granites (a), and andesites, dolerites and Triassic granites (b); field boundaries after Wood (1980).

arcs. The Whitsunday array again contrasts markedly with both the eastern Australian basalt array and high-silica rhyolite field.

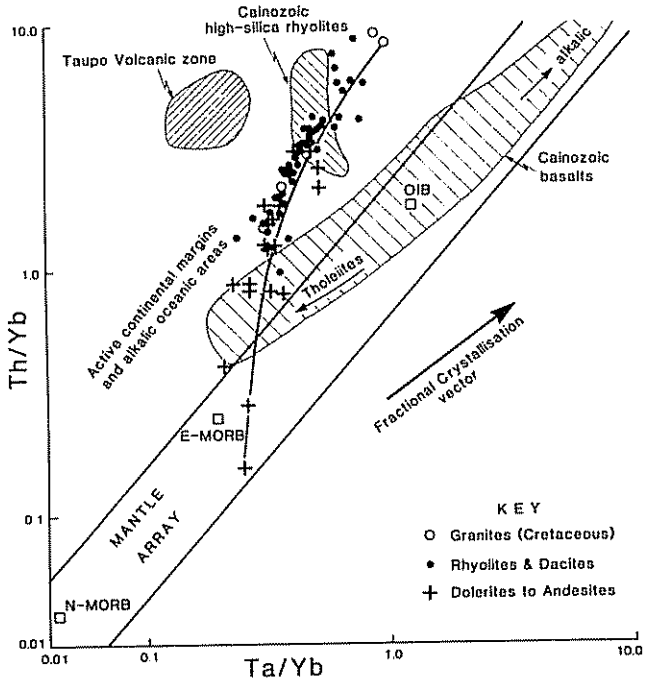

Figure 14 Th/Yb–Ta/Yb for the Whitsunday volcanics and coeval granites, based on plot by Pearce (1983); sources of comparative data as in Figure 12.

8. Isotope geochemistry

Figure 15 plots the Nd and Sr isotopic data for the volcanics and granites. The data are corrected to 115 Ma, except where specific K–Ar or Rb–Sr dates are available (Table 4). Also plotted are comparative fields for the southern New England (Australia) granites, the Cainozoic southern-central Queensland lava field basalts, and the granulite inclusions occurring in these lavas, together with limited data for Carboniferous and Triassic andesites from southern Queensland. Comparison of these data indicates the following points:

(i) The Whitsunday volcanics comprise a coherent data set with ε_{Nd} from +7·3 to +2·2 and initial Sr isotopic ratios from 0·70312–0·70436. The S Molle Is. dolerite, identified as the most primitive sample from trace element data, is among the most isotopically primitive of the data set. The rhyolites lie between ε_{Nd} from +2·2 to +5·7 and I_{Sr} 0·70332–0·70406. The remaining data, however, exhibit overlap between isotopic compositions of the andesites, dacites and rhyolites.

(ii) The Cretaceous granites have ε_{Nd} +6·5 to +3·4, and initial $^{87}Sr/^{86}Sr$ from 0·70312–0·70436, completely overlapping the volcanics, and confirming their comagmatic relationships. The most primitive sample is characterised by extremely abundant dioritic inclusions.

(iii) The Triassic granites are compositionally distinct, with ε_{Nd} +1·5 to +4·2 and initial $^{87}Sr/^{86}Sr$ 0·7116–0·894 (one value at 0·70461), calculated to 115 Ma. These isotopic data thus preclude the Triassic granites as a possible source for the Cretaceous silicic magmas.

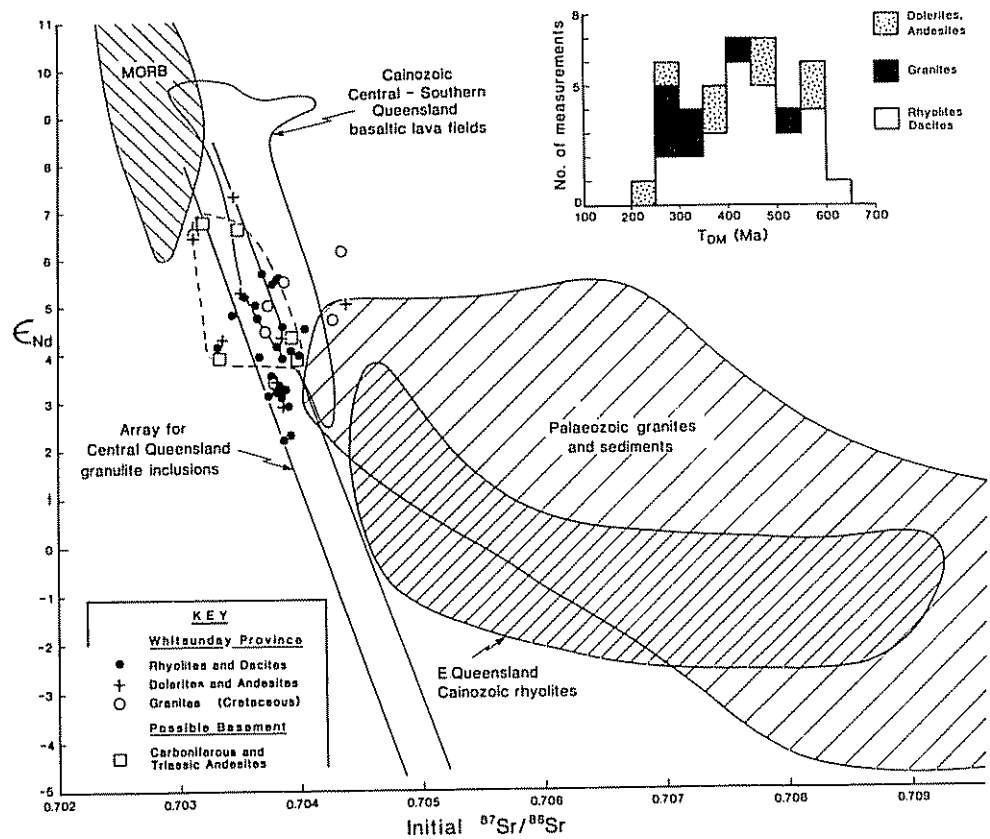

Figure 15 ε_{Nd}-initial $^{87}Sr/^{86}Sr$ ratios for the Whitsunday volcanics; lavas are corrected to 115 Ma, except where specific dates available; inset shows histogram of Nd T_{DM} model ages; comparative data fields presented for modern MORB glasses: Carboniferous and Triassic andesites (Ewart *et al.* 1988, and Table 3, corrected to 115 Ma); granulite inclusion array, (Ewart *et al.* 1988; O'Reilly *et al.* 1988; corrected to 115 Ma); intraplate silicic volcanics and basaltic lava fields (Ewart *et al.* 1988), New England granites (Hensel *et al.* 1985; corrected to 115 Ma).

(iv) The Cretaceous isotopic compositions overlap the fields of the Carboniferous–Triassic andesites, the Cainozoic basalts, and the granulite xenolith array. O'Reilly *et al.* (1988) interpret these inclusions in general as frozen melts, or re-equilibrated cumulates, at the crust–mantle boundary, although inferring that the eastern-central Queensland inclusions reflect interaction between basalt and an older mafic crust with time-integrated Rb and LREE depletion. The critical point with regard to the Cretaceous magmas is that their source(s) are isotopically very similar to the lower crust–lithosphere sources of the Cainozoic basalts and the Carboniferous–Triassic andesites.

The southern New England Batholith granites are generally more radiogenic in Sr than the Cretaceous magmas, implying a different and more evolved source. Palaeozoic–Mesozoic upper crustal sediments are also isotopically precluded as contributing to the Cretaceous magma evolution, noting the Cainozoic silicic magma data field in which such sediments are inferred to have been involved through AFC process (Ewart *et al.* 1988).

Figure 16 further compares the initial Sr isotopic compositions of the southern New England Batholith, the Triassic silicic volcanic provinces of southern Queensland (Stephens 1991), and the Cretaceous suite. Even the least radiogenic of the New England granites (also the least potassic, Shaw & Flood 1981) are mostly more radiogenic than the other two suites. The major significant point, however, is the close correspondence between the Triassic and Cretaceous initial Sr ratios, with the peak of the latter being slightly more radiogenic, possibly reflecting a slight isotopic composition change during the Triassic to Cretaceous interval in a common, or related magma source. If so, then a source Rb/Sr of 0·04–0·08 is implied (consistent with an andesitic source; see below). ε_{Nd} of the Triassic suite ranges from 5·5–2·7, a very similar range to the Cretaceous suite.

The isotopic data thus point to relatively primitive and/or newly accreted, unfractionated source for both the Triassic and Cretaceous magma suites. Stephens (1991) has proposed that the Triassic silicic volcanics originate from

Table 4 Sr and Nd isotopic analyses of the Whitsunday volcanics and granitoids

Sample**	Island location	$^{143}Nd/^{144}Nd^{++}$	$\varepsilon_{Nd(115)}$	$^{147}Sm/^{144}Nd$	Measured $^{87}Sr/^{86}Sr^{++}$	Initial $^{87}Sr/^{86}Sr^{*}$	Rb (ppm)	Sr (ppm)	Rock type	(Anhydrous) SiO_2%
Bo03	Border	0·512768 ± 14	3·52	0·130	0·705989 ± 7	0·70378	88	188	D	70·03
Ca01	Carlisle	0·512776 ± 14	3·89	0·115^{+}	0·704769 ± 10	0·70386	69	358	I	68·78
Cd03	Calder	0·512924 ± 15	6·52	0·132	0·705090 ± 6	0·70312	58	140	G	70·13
Ci01	Cid	0·512766 ± 14	3·41	0·135	0·704167 ± 10	0·70382 (113)	47	623	L	63·02
Cu05	Curlew	0·512839 ± 12	5·00	0·123	0·703759 ± 8	0·70364 (105)	24	842	L	64·34
De12	Dent	0·512809 ± 10	4·45	0·121	0·706177 ± 14	0·70371 (107)	100	178	G	69·41
Dw01	Derwent	0·512866 ± 16	5·51	0·109	0·709947 ± 10	0·70388 (95)	104	67	G	75·29
Es01	Esk	0·512732 ± 12	2·89	0·125^{+}	0·705407 ± 8	0·70392 (125)	97	336	I	69·12
Go05	Goldsmith	0·512791 ± 10	4·06	0·123^{+}	0·709820 ± 2	0·70394	158	127	I	75·33
Ha04	Hayman	—	—	—	0·705912 ± 24	0·70371 (107)	75	150	G	68·70
Ha05	Hayman	—	—	—	0·709788 ± 38	0·70374 (107)	88	64	G	75·75
Hm02	Hamilton	0·512970 ± 10	7·30	0·141	0·703692 ± 12	0·70346	45	899	D	55·14
Hm07	Hamilton	0·512785 ± 10	3·95	0·123	0·716415 ± 34	0·70401 (113)	136	51	L	78·38
Ho03	Hook	0·512757 ± 20	3·35	0·127	0·705461 ± 14	0·70383	99	287	I	70·78
Ho15	Hook	0·512757 ± 16	3·26	0·132	0·706863 ± 13	0·70390	101	161	I	68·26
Ho19/1	Hook	0·512756 ± 12	3·24	0·132^{+}	0·708009 ± 12	0·70385	80	91	I	74·69
Ho29	Hook	0·512811 ± 8	4·32	0·133	0·704710 ± 12	0·70386	70	387	I	62·53
Ho34	Hook	0·512832 ± 14	4·72	0·133^{+}	0·704594 ± 7	0·70366	67	339	D	63·07
Ho39	Hook	0·512790 ± 18	3·93	0·131	0·705696 ± 20	0·70367	117	273	I	64·79
Hs17	Haslewood	0·512696 ± 10	2·21	0·123^{+}	0·709572 ± 8	0·70387 (125)	134	121	I	74·10
In02/2	Ingot	0·512818 ± 10	4·48	0·131	0·704987 ± 8	0·70403 (113)	141	684	L	71·42
Keel	Keelan	0·512863 ± 12	5·69	0·108	0·711605 ± 9	0·70370 (105)	119	65	L	76·74
Kes8	Keswick	0·512865 ± 10	5·45	0·127^{+}	0·705101 ± 8	0·70378 (105)	82	268	L	71·83
Li06	Lindeman	0·512739 ± 16	2·88	0·135	0·704391 ± 29	0·70387 (113)	60	539	L	59·38
Lo11	Long	0·512805 ± 14	4·26	0·128	0·704475 ± 10	0·70337 (110)	83	339	L	62·92
Mp16	Middle Percy	0·512840 ± 10	5·00	0·124	0·705537 ± 7	0·70440	57	235	D	60·57
No02	Noel	0·512831 ± 14	4·99	0·113^{+}	0·704913 ± 10	0·70375 (107)	115	435	G	64·08
Pe01	Pentecost	0·512695 ± 18	2·31	0·115^{+}	0·704589 ± 11	0·70393	53	356	I	71·60
Pr01	Prudhoe	0·512859 ± 10	5·28	0·131	0·703888 ± 16	0·70352	47	610	D	60·60
Sm08	South Molle	0·512791 ± 12	4·13	0·119	0·730512 ± 21	0·70332 (100)	162	27	L	75·33
Sm10	South Molle	0·512858 ± 16	5·19	0·135	0·706731 ± 18	0·70355 (110)	83	118	L	71·92
Sm11	South Molle	0·512929 ± 14	6·44	0·145	0·703287 ± 36	0·70312 (110)	20	551	D	50·07
Sc04	Scawfell	0·512808 ± 14	4·70	0·103^{+}	0·709775 ± 11	0·70429 (117)	143	125	G	74·68
Sh08	Shaw	0·512798 ± 12	4·15	0·126	0·706791 ± 48	0·70382 (113)	122	191	L	72·93
Sh09	Shaw	0·512744 ± 14	3·09	0·127	0·705289 ± 10	0·70386	83	274	D	71·32
Sh10	Shaw	0·512731 ± 16	3·10	0·109	0·705907 ± 59	0·70375	83	182	D	76·55
Sh25	Shaw	0·512741 ± 18	3·19	0·116^{+}	0·709328 ± 14	0·70381 (113)	183	154	L	73·50
TP01	Tinonee Peak	0·512857 ± 20	5·57	0·108^{+}	0·705319 ± 11	0·70384 (105)	55	160	L	74·11
TP07	Tinonee Peak	0·512855 ± 18	5·53	(0·108)	0·706453 ± 10	0·70382 (105)	86	141	L	77·58
Tr01	Three Rocks	0·512882 ± 18	6·14	(0·103)	0·709973 ± 11	0·70436 (117)	137	117	G	75·99
Wg01	Wigton	0·512760 ± 14	3·38	0·129^{+}	0·705202 ± 8	0·70380 (116)	83	282	G	68·37
Triassic Andesites (Neara Volcanics)										
37958		0·512775 ± 11	3·88	0·115	0·703705 ± 11	0·70334	79	1042		
37967		0·512939 ± 14	6·61	0·145	0·703621 ± 23	0·70349	24	754		
38645		0·512803 ± 16	4·31	0·112	0·704771 ± 12	0·70394	89	552		

Notes: $^{++}$ quoted uncertainties are ±2se; analyses performed at Sirotope, C.S.I.R.O., North Ryde. $^{147}Sm/^{144}Nd$ calculated from isotope dilution data, except samples with $^{+}$ (neutron activation), and figures in brackets (inferred), * calculated for 115 Ma except where indicated otherwise (see Table 1). D = dykes; G = granites; I = ignimbrites; L = lava flows. ** See Section 11 for University of Queensland rock collection numbers.

partial melting of an andesitic crust of early Triassic (or older) age. It is proposed here that a plausible source may be partial melting of mixed igneous and sediment components of the Permo–Triassic arc crust. The geographic plausibility of this is illustrated in Figure 17, in which the zones of both Permian and Triassic volcanism and plutonism are seen to run obliquely to the present coast, and are thus intersected by the zone of Cretaceous rifting. It is therefore expected that remelting of the older Mesozoic crust should contribute to Cretaceous magma genesis. The relatively primitive isotopic compositions of the Triassic and Cretaceous volcanics in the central Queensland region also implies an absence of an older, more geochemically evolved crust being present beneath the Permo–Triassic arcs, and strengthens the view for the progressive lateral accretion of the eastern Queensland crust by arc migration, at least to the early Mesozoic (e.g. Veevers *et al.* 1991). The involvement of Mesozoic to Palaeozoic crust in the Cretaceous magma genesis also receives support from the Nd model T_{DM} ages (inset, Fig. 15), most of which lie between 250–600 Ma.

9. Discussion

The trace element data point toward two main processes operating in the evolution of the Whitsunday magmas: (i) Two component mixing, one end-member inferred to be a within-plate tholeiitic magma (near E-type MORB), the second a silicic magma inferred to be rhyolitic, presumably low-silica rhyolite. (ii) Fractional crystallisation superimposed on the mixing trends, being especially pronounced in the high-silica rhyolites. These processes are interpreted to have produced the overall continuity of magma compositions from mafic to felsic. The trace element data also reveal the Cretaceous granites to be geochemically indistinguishable from the silicic volcanics.

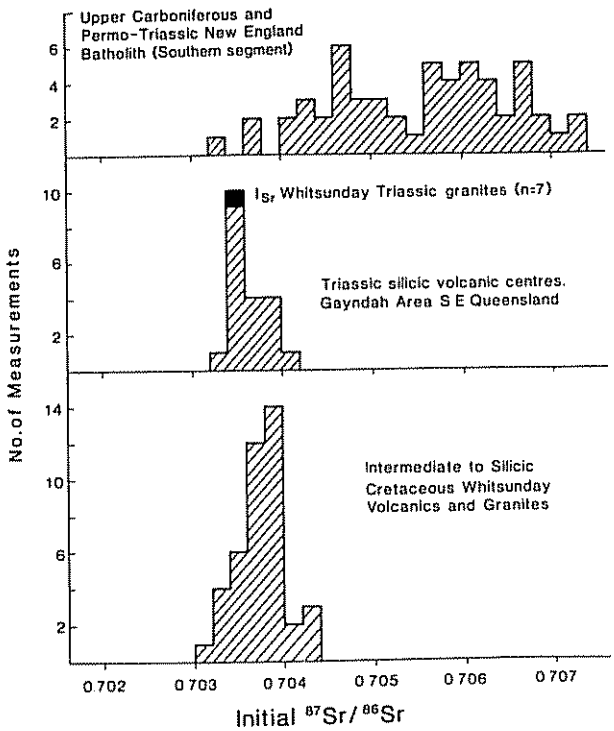

Figure 16 Histograms comparing the initial Sr isotope ratios of the southern New England Batholith (Shaw & Flood 1981), the central Queensland Triassic silicic volcanic centres (Gayndah region; Stephens 1991), and the Whitsunday Volcanics and granites (this paper).

The isotopic data clearly imply the involvement of a juvenile crust and lithosphere, the former being interpreted as most plausibly Permo–Triassic arc crust. Partial refusion of this crust is here inferred to have produced low-silica rhyolites, the remelting process developing in response to basaltic magma injection from upwelling lithosphere and asthenosphere. In fact, such remelting may also involve in part remelting of restite developed during the Triassic phase of volcanism, as Triassic granites are locally present underlying the Whitsunday volcanic region, as described. Triassic rhyolites also occur on the adjacent mainland (Conway Peninsula, Fig. 1). A plausible tectonic model is passive continental margin extension by detachment faulting (e.g. Lister & Etheridge 1989).

It is therefore proposed that the Whitsunday magmatism represents a calc-alkaline to high-K magma suite produced as a consequence of a divergent, rather than convergent plate margin. The development of intermediate magma compositions is interpreted to result largely from mixing processes, with superimposed fractional crystallisation. The "arc-like" signatures identified within the suite, especially in the intermediate to silicic compositions, are interpreted to be inherited from the Mesozoic arc source, through the production of rhyolitic magmas. Mixing of these magmas

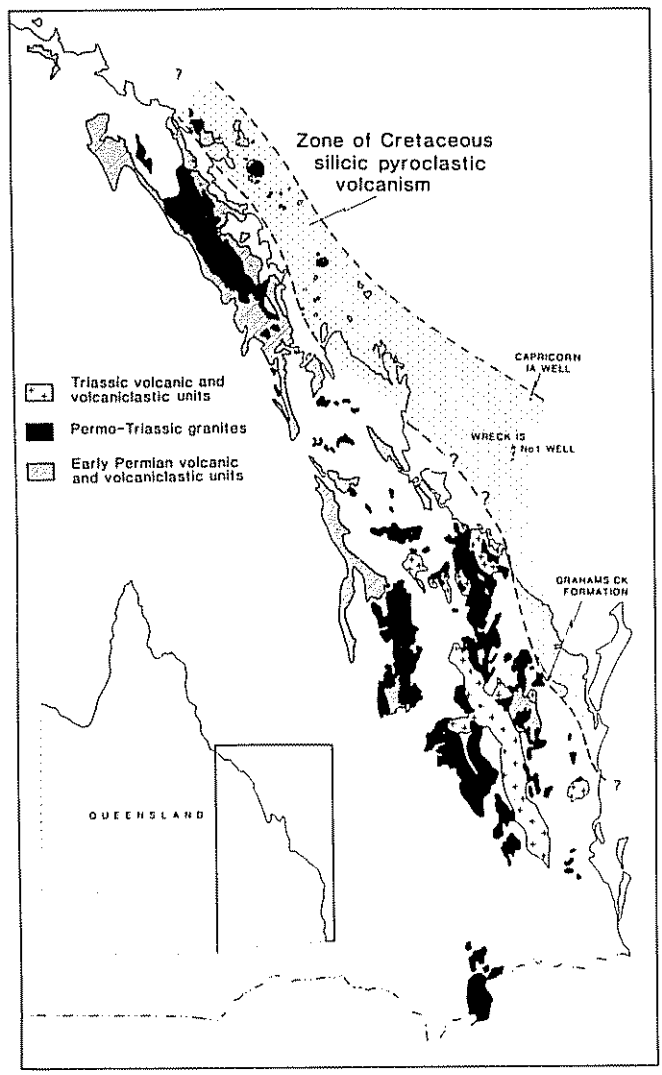

Figure 17 Map illustrating the generalised distribution in central and southern Queensland of Permian and Triassic volcanic and volcaniclastic units, and Permo-Triassic granites, in relation to the inferred distribution of the Cretaceous volcanic rift zone (see also Clarke *et al.* 1971); geological boundaries after Day *et al.* (1983).

with lithosphere-derived tholeiites has allowed these "arc" signatures to be transferred through much of the Whitsunday magma suite. Mixing is interpreted to dominantly involve magma mixing. The data of Frost and Mahood (1987) indicate that efficient mixing is only likely if either compositional differences between host and injected mafic magma are less than 10% SiO_2, or if the mass fraction of mafic magma exceeds approximately 0·5. The resulting mixed magmas correspond to tonalites to mafic granodiorites, i.e. corresponding to the compositions of the inclusions within some of the Cretaceous granites. The more silicic compositions are thus likely to represent localised magma mingling and assimilation with superimposed fractional crystallisation. The latter has demonstrably occurred, especially in the high silica rhyolites. It is also significant to recall the more complete continuity of rock compositions within the dykes (Fig. 6), perhaps reflecting more efficient mechanical stirring during dyke emplacement.

On a regional scale, as previously noted, Cretaceous volcanism was almost certainly originally more widespread along the eastern Australian coast, possibly now downfaulted along the continental shelf. In the context of the southwestern Pacific, Cretaceous volcanism occurs in New Zealand, the Lord Howe Rise, and New Caledonia (Fig. 18). In New Zealand, volcanic products of similar age (89 Ma) to the Whitsundays are found only in the Mt Somers region (Barley 1987). They range from basaltic andesite to high-silica rhyolite, with medium to high-K affinities. The rhyolites are peraluminous, and are interpreted by Barley (1987) to be partial melts of the quartzo-feldspathic Torlesse sediments (i.e. a more "mature" and more radiogenic source than that of the Whitsunday magmas). The intermediate composition is explained by AFC processes involving mantle derived tholeiites. Volcanicity is correlated with a change from compressional to extensional tectonic regimes after the Rangitata orogeny.

Cretaceous rhyolitic pyroclastics and lavas are present on the southern part of the Lord Howe Rise, recovered at the base of the DSDP Hole 207 (Burns *et al.* 1973; McDougall & van der Lingen 1974). Bimodal Cretaceous volcanism occurs extensively along the length of New Caledonia, part of the Norfolk Ridge (Paris 1981), and includes abundant rhyolitic and rhyodacitic tuffs interbedded in thick sediment sequences in the Noumea and Diahot basins (65–75 Ma). These widespread, although apparently localised, occurrences of Cretaceous silicic volcanism are thus of considerable significance in terms of the Cretaceous fragmentation of the eastern Australasian continent; the submarine Lord Howe and Norfolk ridges are regarded as rifted fragments of the former continent (e.g. Kroenke 1984). Of particular further interest is the recent recovery of pre-Upper Eocene rhyolites (exact age not yet known) in the lower 210 m of ODP Hole 841 on the Tonga forearc (ODP Leg 135 Scientific Party 1991), raising speculation that the Tonga and Lau ridges may also represent the easternmost rifted fragments of the former continental margin.

It is thus possible that rhyolitic volcanism accompanying the Cretaceous regional fragmentation was originally widespread in the southwestern Pacific, but is now largely buried in the off-shore ridges, and on the continental shelves. If so, the rhyolites will have sampled, by partial melting, segments of the former eastern Australasian continental margin of various ages and in various stages of evolution.

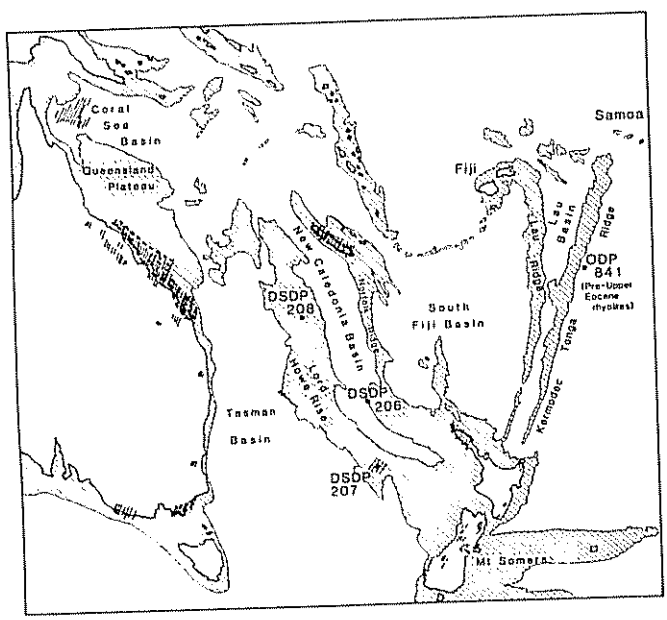

Figure 18 Map of southwestern Pacific illustrating the generalised distribution of continents and continental shelves, islands, and submarine ridges (based on 2000 m bathymetric contour), and showing the general distribution of inferred, drilled, and exposed Cretaceous volcanic and intrusive provinces.

10. Acknowledgements

This project was funded by an Australian Research Council grant, including post-doctoral position to RWS. All neutron activation analyses were carried out in the Department of Geology, Australian National University. Valuable field assistance was given by C. J. Stephens, A. Faulkner, and P. Colls, while much laboratory assistance was provided by F. Audsley and R. Hall (University of Queensland) and Dr D. J. Whitford and S. Craven (Sirotope, CSIRO). Stimulating discussion with J. Parianos, S. Bryan, and P. Downes, each completing theses on the region, are acknowledged. Dr S. D. Weaver and an anonymous reviewer provided helpful comments on the manuscript.

11. Note added in proof

The following are the University of Queenslnd official departmental museum numbers for the samples included in Table 4. UQ number is in parenthesis after sample.

Bo03 (49247), Ca01 (49269), Cd03 (49274), Ci01 (49275), Cu05 (49300), De12 (49312), Dw01 (49331), Es01 (49332), Go05 (49342), Ha04 (49346), Ha05 (49347), Hm02 (49356), Hm07 (49361), Ho03 (49378), Ho15 (49391), Ho19/1 (49396), Ho29 (49407), Ho34 (49412), Ho39 (49419), Hs17 (49477), In02/2 (49418), Keel (49484), Kes8 (49496), Li06 (49525), Lo11 (49555), Mp16 (49571), No02 (49575), Pe01 (49576), Pr01 (49597), Sm08 (49619), Sm10 (49621), Sm11 (49622), Sc04 (49640), Sh08 (49650), Sh09 (49651), Sh10 (49652), Sh25 (49667), TP01 (49702), TP07 (49708), Tr01 (49709), Wg01 (49726).

12. References

Barley, M. E. 1987. Origin and evolution of Mid-Cretaceous, garnet-bearing, intermediate and silicic volanics from Canterbury, New Zealand. J. VOLCANOL. GEOTHERM. RES. **32**, 247–67.

Blundy, J. D. & Holland, T. J. B. 1990. Calcic amphibole equilibria and a new amphibole–plagioclase geothermometer. CONTRIB. MINERAL. PETROL. **104,** 208–24.

Burns, R. E. & Andrews *et al.* 1973. *Initial Reports of the Deep Sea Drilling Project, Washington (U.S. Government Printing office)* **21,** 197–269.

Clarke, D. E., Paine, A. G. L. & Jensen, A. R. 1971. Geology of the Proserpine 1:250,000 Sheet area, Queensland. BUR. MINER. RES. GEOL. GEOPHYS. REP. **144.**

Davies, P. J. & Marshall, J. F. (in press). The Great Barrier Reef—evolution and growth. SPEC. PUB. INT. ASSOC. SEDIMENTOL.

Day, R. W., Whitaker, W. G., Murray, G. C., Wilson, I. H. & Grimes, K. G. 1983. Queensland geology. A companion guide to the 1:250,000 scale geological map (1975). GEOL. SURV. QUEENSLAND PUB. **383.**

Ellis, P. L. & Whitaker, W. G. 1976. Geology of the Bundaberg 1:250,000 sheet area. GEOL. SURV. QUEENSLAND REP. **90.**

Etheridge, M. A. & Lister, G. S. 1987. Extensional models for passive margin evolution. *In Extended Abstracts—Applied Extension Tectonics, Bureau Mineral Resources Record 1987/51,* 87–94.

Ewart, A. 1979. A review of the mineralogy and chemistry of Tertiary–Recent dacitic, rhyolitic, and related salic volcanic rocks. *In* Barker, F. (ed.) *Trondhjemites, dacites and related rocks,* 13–121. Amsterdam: Elsevier.

Ewart, A. 1982. The mineralogy and petrology of Tertiary–Recent orogenic volcanic rocks: with special reference to andesitic–basaltic compositional range. *In* Thorpe, R. S. (ed.) *Andesites,* 25–95. New York: Wiley.

Ewart, A. & Chappell, B. W. 1989. Trace element geochemistry. *In* Johnson, R. W. (ed.) *Intraplate volcanism in Eastern Australia and New Zealand,* 219–35. Cambridge: Cambridge University Press.

Ewart, A., Chappell, B. W. & Menzies, M. A. 1988. An overview of the geochemical and isotopic characteristics of the Eastern Australian Cainozoic volcanic provinces. J. PETROL. SPEC. LITHOSPHERE ISSUE, 225–73.

Falvey, D. A. & Middleton, M. F. 1981. Passive continental margins; evidence for a pre-breakup deep crustal metamorphic subsidence mechanism. *Oceanol. Acta, Proc. 26th Intern. Geol. Congress, Geology of continental margins symposium, Paris,* 7–17 July, 1980, 103–14.

Falvey, D. A. & Mutter, J. C. 1981. Regional plate tectonics and the evolution of Australia's passive continental margins. BMR J. GEOL. GEOPHYS. **6,** 1–29.

Frost, T. P. & Mahood, G. A. 1987. Field, chemical, and physical constraints on mafic–felsic magma interaction in the Lamarck Granodiorite, Sierra Nevada, California. GEOL. SOC. AM. BULL. **99,** 272–91.

Green, D. C. & Webb, A. W. 1974. Geochronology of the northern part of the Tasman geosyncline. *In* Denmead, A. K., Tweedale, G. W. & Wilson, A. F. (eds), *The Tasman Geosyncline—A symposium,* 275–93. Brisbane: Geological Society of Australia, Queensland Division.

Henderson, R. A. 1980. Structural outline and summary geological history for northeastern Australia. *In* Henderson, R. A. & Stephenson, P. J. (eds) *The geology and geophysics of northeastern Australia,* 1–26. Brisbane: Geological Society of Australia, Queensland Division.

Hensel, H. D., McCulloch, M. T. & Chappell, B. W. 1985. The New England Batholith; constraints on its derivation from Nd and Sr isotopic studies of granitoids and country rocks. GEOCHIM. COSMOCHIM. ACTA **49,** 369–84.

James, R. S. & Hamilton, D. L. 1969. Phase relation in the system $NaAlSi_3O_8$–$CaAl_2Si_2O_8$ at 1 Kilobar water vapour pressure. CONTRIB. MINERAL. PETROL. **21,** 111–41.

Jensen, A. R., Gregory, C. M. & Forbes, V. R. 1966. Geology of the Mackay 1:250,000 Sheet area, Queensland. BUR. MINER. RES. GEOL. GEOPHYS. REP. 104.

Kroenke, L. W. 1984. Cenozoic tectonic development of the Southwest Pacific. UN ESCAP, CCOP/SOPAC TECH. BULL. **6.**

Le Maitre, R. W. (ed.) 1989. *A classification of igneous rocks and glossary of terms. Recommendations of the International Union of Geological Sciences Subcommission on the systematics of igneous rocks.* Oxford: Blackwell.

Lister, G. S., Etheridge, M. A. & Symonds, P. A. 1988. Extension history of the margins of the Tasman Sea. *Abstracts, No. 21, Ninth Aust. Geol. Convention, February 1–5, 1988, Brisbane,* 252–3.

Lister, G. S. & Etheridge, M. A. 1989. Detachment models for uplift and volcanism in the Eastern Highlands, and their application to the origin of passive margin mountains. *In* Johnson, R. W. (ed.) *Intraplate Volcanism in Eastern Australia and New Zealand,* 297–313. Cambridge: Cambridge University Press.

McDougall, I. & van der Lingen, G. J. 1974. Age of the rhyolites of the Lord Howe Rise and the evolution of the southwest Pacific Ocean. EARTH PLANET. SCI. LETT. **21,** 117–26.

Nekvasil, H. 1988. Calculated effect of anorthite component on the crystallization paths of H_2O-undersaturated haplogranitic melts. AM. MINERAL. **73,** 966–82.

ODP Leg 135 Scientific Party 1991. A new view of arc/backarc systems. GEOTIMES **36(8),** 19–20.

O'Reilly, S. Y., Griffin, W. L. & Stabel, A. 1988. Evolution of Phanerozoic Eastern Australian lithosphere: Isotopic evidence for magmatic and tectonic underplating. J. PETROL. SPEC. LITHOSPHERE ISSUE, 89–108.

Paris, J.-P. 1981. Geologie de la Nouvelle-Calédonie. BUR. RECHERCHES GEOL. MIN. **113.**

Pearce, J. A. 1983. Role of the sub-continental lithosphere in magma genesis at active continental margins. *In* Hawkesworth, C. J. & Norry, M. J. (eds) *Continental basalts and mantle xenoliths* 230–49. Orpington: Shiva.

Shaw, S. E. & Flood, R. H. 1981. The New England Batholith, Eastern Australia: geochemical variations in space and time. J. GEOPHYS. RES. **86,** 10,530–44.

Smart, J. & Senior, B. R. 1980. Jurassic–Cretaceous basins of northeastern Australia. *In* Henderson, R. A. & Stephenson, P. J. (eds) *The geology and geophysics of northeastern Australia,* 315–28. Brisbane: Geological Society of Australian, Queensland Division.

Stephens, C. J. 1991. *The Mungore Cauldron and Gayndah Centre. Late Triassic large-scale silicic volcanism in the New England Fold Belt near Gayndah, southeast Queensland.* Unpublished Ph.D. Thesis, University of Queensland, Brisbane.

Sun, S.-S. & McDonough, W. F. 1989. Chemical and isotopic systematics of oceanic basalts. *In* Saunders, A. D. & Norry, M. J. (eds) *Magmatism in the ocean basins,* 313–45. GEOL. SOC. SPEC. PUBL. **42.**

Symonds, P. A., Fritsch, J. & Schluter, H.-U. 1984. Continental margin around the western Coral Sea Basin: Structural elements, seismic sequences, and petroleum geological aspects. *In* Watson, S. T. (ed.) *Trans. Third Circum-Pacific Energy & Mineral Resources Conf., Hawaii,* 243–52. Tulsa: American Association of Petroleum Geologists.

Symonds, P., Davies, P. J., Feary, D. A. & Pigram, C. J. 1988. Geology of the northeastern Australian margin basins. *In* PESA (Qld)—ODCAA SPE Petroleum Symp., Queensland 1988; Exploration Development: 61–77.

Symonds, P. A. & Willcox, J. B. 1989. Australia's petroleum potential in areas beyond an Exclusive Economic zone. BMR J. AUST. GEOL. GEOPHYS. **11,** 11–36.

Veevers, J. J. (ed.) 1984. *Phanerozoic earth history of Australia.* Oxford: Clarendon Press.

Veevers, J. J., Powell, C. McA. & Roots, S. R. 1991. Review of seafloor spreading around Australia. I. Synthesis of the patterns of spreading. AUST. J. EARTH SCI. **38,** 373–89.

Webb, A. W. & McDougall, I. 1968. The geochronology of the igneous rocks of Eastern Queensland. J. GEOL. SOC. AUST. **15,** 313–46.

Wood, D. A. 1980. The application of a Th–Hf–Ta diagram to problems of tectonomagmatic classification and to establishing the nature of crustal contamination of basaltic lavas of the British Tertiary volcanic province. EARTH PLANET. SCI. LETT. **50,** 11–30.

A. EWART and R. W. SCHON, Department of Earth Sciences, University of Queensland, St. Lucia, Queensland 4072, Australia.

B. W. CHAPPELL, Department of Geology, Australian National University, Canberra, A.C.T. 2601, Australia.